Noise Figure Measurements

Theory and Application

Contents

1. Introduction

A list of essential measurements in electronic circuits and systems would probably include *voltage*, *current*, *power*, and *distortion*. An even more complete list should also include the measurement of *noise*. When assessing the dynamic range of a single electronic component or an entire electronic system, distortion and maximum power bound the high side of the dynamic range performance and noise bounds the low side. The measurement of noise is a fundamental requirement for electronic design.

Noise in electronic systems is a noticeable phenomenon in applications such as broadcast radio, weather radar, avionics radar, and audio to name a few. Shannon's channel capacity theorem which governs the amount of information that can be transmitted over a communications channel is bounded by noise. Increasing channel capacity is all about increasing the signal-to-noise ratio of the information in the transmitter/receiver chain. Regulatory restrictions on the amount of transmit power increases the importance of noise management in support of higher data rates. Bit error rate and error vector magnitude are metrics used to assess that quality of digitally modulated signals. Among the terms that can degrade these figures of merit is noise.

Being an essential consideration in the design of electronic systems, one would think most design engineers should have a good grasp on measuring noise and mitigating its effects in their systems. However, in general, this is not the case as noise is an elusive subject to understand. Dealing with noise requires dealing with statistics, probability distribution functions, coherence versus independence, and a whole list of jargon that most engineers maybe once knew during their studies. Any brave soul who has endured tedium of analyzing analog system noise is probably not extremely anxious to perform these calculations again. With the uncomfortable nature of statistics governing the math involved in noise analysis and the tedium of performing this analysis on analog circuits, noise is more often than not neglected in design work.

Fortunately in RF design, engineers have tools that remove some of the mystery and tedium associated with the analysis and measurement of noise. The concept of *noise figure* is one of those tools. This application note serves as a tutorial in understanding, applying and measuring noise figure. A primary focus is how noise figure applies particularly to RF circuits and systems. The treatment of noise calculations in mixed impedance designs associated with analog circuits and systems is not highlighted in this application note.

This application note covers a few major themes. First, it reviews the generation of noise in electronic devices, leading to the theoretical treatment of noise in a more complex electronic system. The second section discusses the measurement of noise figure using the Y-factor measurement method is discussed. Next, the calculation of the measurement uncertainty of the Y-factor noise figure measurement is analyzed, showing sources of measurement uncertainties and best practices to minimize these uncertainties. The final section focuses on the cold-source noise figure measurement technique, by outlining a particular measurement method and its corresponding measurement uncertainty.

2. Defining Noise

Noise is a very broad topic so it is important to clearly state which disturbances are and which ones are not included in the calculation of noise figure. Once this is established, this section defines how broadband noise is generated. Gaining this insight allows you to consider the environmental and measurement conditions that may affect the level of the noise generated.

Electromagnetic Interference

The textbook definition of noise is *any* unwanted disturbance that interferes with the operation of any system. In electronic systems, one source of noise that fits this definition is electromagnetic interference. Figure 2.1 illustrates some of the forms of electromagnetic interference.

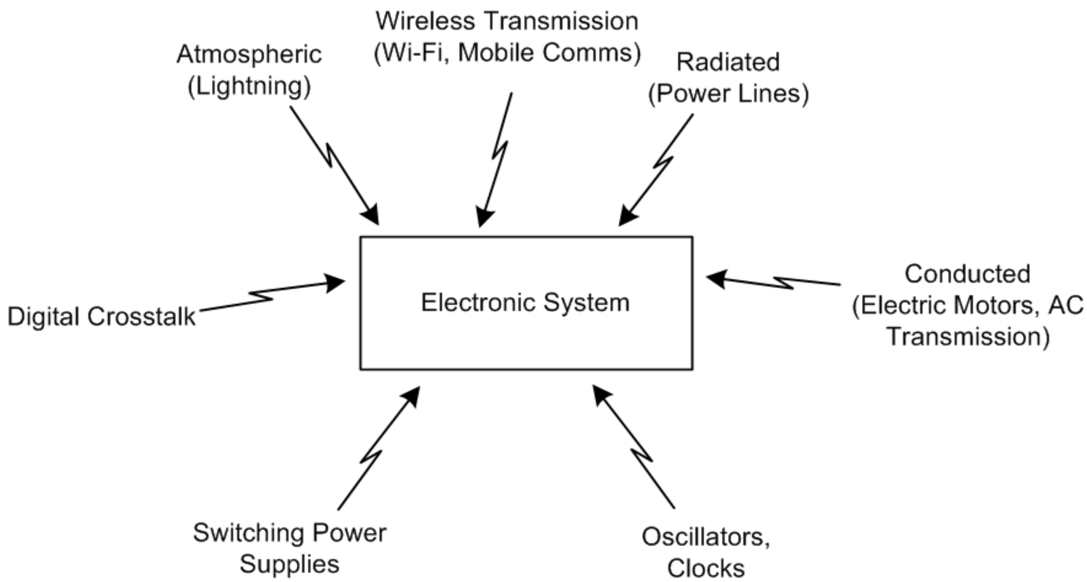

Figure 2.1 Sources of Electromagnetic Interference

Electromagnetic interference (EMI) consists of both radiated and conducted energy, most often narrowband in frequency. Sources of EMI stem from electronic circuits and systems both within and outside the circuit of interest. Design techniques such as shielding, filtering, and separation of coupled lines in printed circuit layout assist in minimizing electromagnetic disturbance.

While EMI is an extremely important consideration, this topic is not covered in this application note. This wide area of design information can be found in references such as [1].

Intrinsic Noise

The other important category of electronic disturbance is electrical noise generated by electronic devices such as resistors and semiconductors. This so-called *intrinsic noise* results from the fact that at the sub-atomic level, voltage and current are not steady, but rather chaotic in nature. One form of intrinsic noise results from agitation of electrons in a resistive material with the energy level of this agitation directly proportional to temperature. Another form of intrinsic noise is a consequence of current flow through semiconductors. Semiconductor material in forward bias consists of random, packetized carrier concentrations about an average value. The random portion reveals itself as noise.

Intrinsic noise sets a lower limit on the amplitude of a signal that can be transmitted or received with an acceptable level of signal quality. Intrinsic noise is most often wideband in frequency, affecting signals that span a wide frequency spectrum. Once intrinsic noise enters a system, further amplification merely increases both signal and noise levels, which does nothing to improve signal quality. Understanding how to minimize noise in the transmit or receive paths of an electronic system normally is the best course of action to the improvement of signal integrity. Above all, knowing how to accurately measure intrinsic noise is a requirement at both the component and system level. This is a major focus of this application note.

To assist in mitigating the effects of noise in an electronic system, it is first instructive to understand the sources of various forms of intrinsic noise. Awareness of the source of noise can lead to ideas on how to minimize the amount of noise in a circuit or system.

Thermal Noise

Any resistive material, be it an actual resistor or the resistivity of a conductor, generates a small, but measurable amount of electrical power. This power originates from the random thermal motion of electrons in the resistive material. The magnitude of the power level is unaffected by the presence of direct current in the material. This so-called *thermal noise*, or historically *Johnson noise* [2], has a power level directly proportional to temperature.

When measuring the voltage across a resistance, the instantaneous value of the voltage follows a Gaussian probability distribution function with a mean value of zero volts as shown in Figure 2.2.

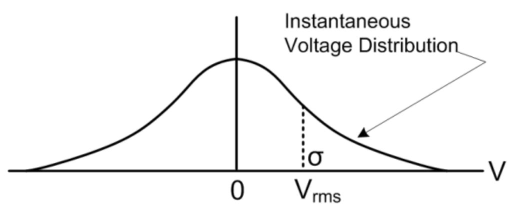

Figure 2.2 Thermal Noise Voltage Distribution

Instantaneous voltage can be defined only using statistical probability; it is not a constant value. To analyze voltage noise in a circuit, the root-mean-square (rms) value of the voltage is commonly used. Equation (2-1) defines the rms value of the instantaneous voltage, *v(t)*.

$$V_{rms} = \sqrt{\frac{1}{T}\int_0^T v^2(t)\,dt} \qquad (2\text{-}1)$$

The instantaneous square of the voltage is integrated over a finite period of time, T. Defined in this manner, V_{rms} is one standard deviation of the Gaussian voltage distribution as shown in Figure 2.2. Average power, which noise power uses in its definition, when measured across a resistor, R, relates to rms voltage using Equation (2-2).

$$P_{avg} = \frac{V_{rms}^2}{R} \qquad (2\text{-}2)$$

Using rms voltages and currents when calculating noise power levels is not only convenient, but also a necessity. Using instantaneous voltages and currents, as applied to the analysis of electronic circuits, is not the correct approach for the analysis of noise.

Unfiltered thermal noise has constant average power versus frequency as shown in Figure 2.3.

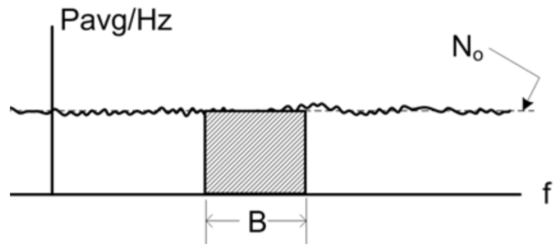

Figure 2.3 Noise Power Spectral Density

Power spectral density is frequency normalized average power given in units of watts per hertz. If the power spectral density of noise is N_o in a system with bandwidth, B, then the average noise level is N_oB. This demonstrates that the average noise power depends on the bandwidth of the measurement system. The wider the bandwidth, the larger the average noise power of the system. When the power spectral density is constant over all frequencies of interest, this is commonly referred to as *white noise*. The term white because noise has energy over all frequencies just as white light is a combination of all frequencies in the visible spectrum.

For convenience, a resistor with noise power can be equated to a noiseless resistor in either a Thevenin or Norton equivalent noise generator realization as shown in Figure 2.4 [3].

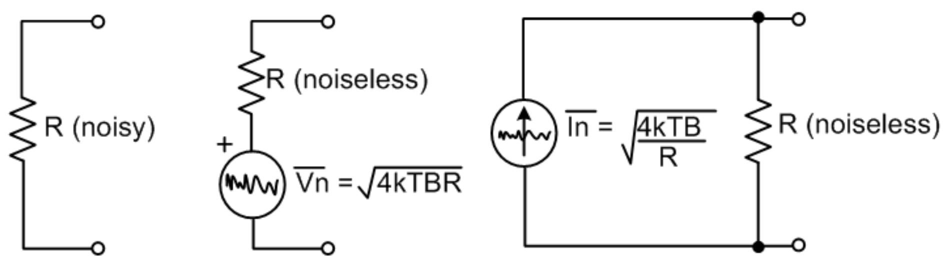

Figure 2.4 Thermal Noise Generator Models

The open-circuit rms voltage across the resistor is $\overline{v_n} = \sqrt{4kTBR}$. Boltzmann's constant, k, is 1.3806 x 10^{-23} joules/kelvin and temperature, T, is given in units of kelvin. The value B is the noise power bandwidth of the system in units of hertz. Most often these rms noise voltage and current values use 1 Hz bandwidth and are described in units of voltage per root Hz and amps per root Hz respectively. Table 2.1 shows some rms voltage and noise values versus resistance, R, at a temperature of 290 K (16.85 °C or 62.3 °F).

R [Ω]	$\overline{v_n}$ $[nV/\sqrt{Hz}\,]$	$\overline{I_n}$ $[pA/\sqrt{Hz}\,]$
50	0.89	17.9
100	0.63	12.66
1 k	2.0	4.0
10 k	6.33	1.27
100 k	20.01	0.4

Table 2.1 RMS Noise Voltage and Current versus R at T=290 K

These values are unusually small quantities, indicating the difficulty in the measurement of noise.

Maximum power transfer for a real impedance device, for instance purely resistive material, occurs when the device is connected to an equal value load resistance. Under this condition, this maximum transferred power is referred to as the device's *available power*. Connecting the Thevenin equivalent noise voltage generator for resistance R to a load resistance R_L = R as shown in Figure 2.5 allows for the calculation of available power from the noisy resistor R.

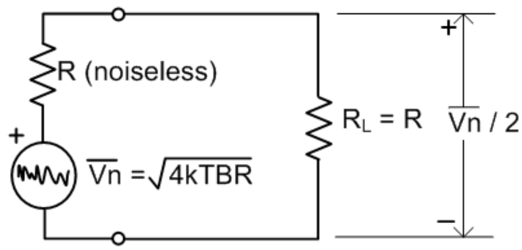

Figure 2.5 Circuit Diagram for Available Noise Power

Note that in this calculation, the noise generator of the load resistor is not considered. The available power from source resistor R is the only consideration. Available power from the source is designated as P_{avs}:

$$P_{avs} = \frac{V_{rms}^2}{R_L} = \frac{\overline{v_n^2}}{4R} = kTB \tag{2-3}$$

T is the resistor's body temperature in units of Kelvin. Notice that available power is independent of the resistor value. With temperature equal to 290 K, $P_{avs} = 4 \times 10^{-21}$ W/Hz and $10\log_{10}(P_{avs})$ is the familiar -174 dBm/Hz (-173.98 dBm/Hz to be more precise). The per hertz designation shows that this power value is power spectral density and that actual noise power scales with bandwidth. Every factor of 10 change in the bandwidth changes P_{avs} by 10 dB.

Shot Noise

Shot noise results from direct-current (DC) flow and is associated primarily with semiconductor devices [3]. Current across any PN junction such as those found in diodes, CMOS junctions and bipolar junctions contribute to shot noise. Basic semiconductor theory shows that current is the transfer of electrons from the N type region to the P type region when there is sufficient potential voltage across the PN barrier. Electrons in the N region filling holes in the P region is a random process. Total current consists of an average DC term plus a noise term whose rms value is described by (2-4).

$$\overline{I_n} = \sqrt{2qI_{DC}B} \tag{2-4}$$

The term q is the electronic charge (1.6×10^{-19} Coulombs) and I_{DC} is the average DC value in the semiconductor junction. So, shot noise power increases as a function of the DC – devices that require more current, have higher shot noise. This is a reason why preamplifiers, for which a low noise characteristic is an important consideration, generally have lower bias currents than power amplifiers.

Similar to thermal noise, shot noise also possesses a Gaussian probability distribution function. The mean-value of the noise, however, is I_{DC}.

Other Noise Generators

Flicker noise results from contaminants and crystal defects in the semiconductor material [3]. Its noise power is inversely proportional to frequency. That is, flicker noise has higher power levels at lower frequencies as depicted in Figure 2.6. When plotted on a logarithmic frequency scale, flicker noise, or 1/f noise, has a linear slope.

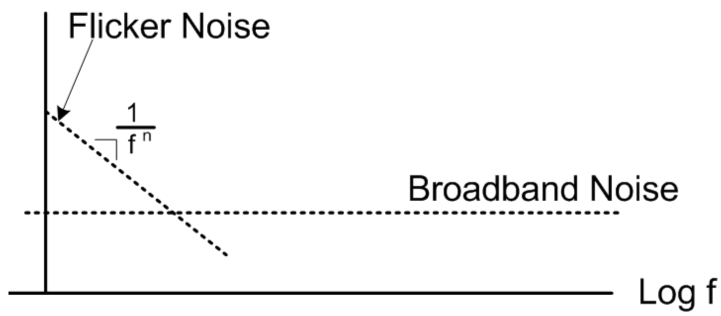

Figure 2.6 Flicker Noise

Flicker noise is especially important for low-frequency preamplifiers. Oscillators in particular must contend with this form of noise as this noise modulates onto the oscillator signal showing up as an offset noise surrounding the carrier. This form of noise has a non-Gaussian probability distribution function.

Burst noise, sometimes referred to as popcorn noise, is found in active devices such as semiconductors. The source of this noise is not fully understood, but appears to be related to contamination in the device material [3]. This noise can superimpose as bumps on the straight line flicker noise curve when plotted on a log-frequency scale as shown in Figure 2.7.

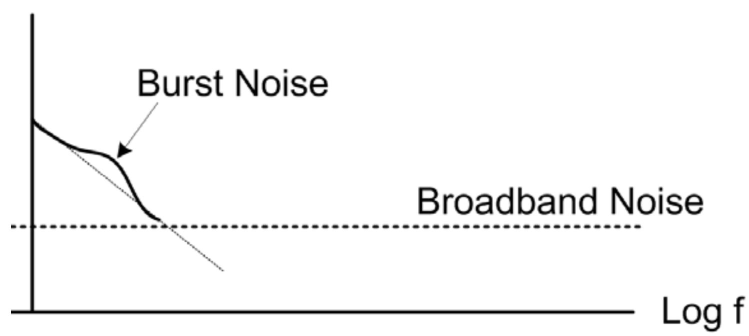

Figure 2.7 Burst Noise

This form of noise also does not possess a Gaussian probability distribution function.

Avalanche noise is generated when a semiconductor PN junction is reverse biased with sufficient voltage to cause breakdown. Zener diodes operate in this manner. For the measurement of RF noise figure, Zener diode avalanche noise is exploited to create a calibrated noise source. This form of noise is also non-Gaussian, but it does have a relatively flat spectral density versus frequency over a very wide bandwidth.

3. Circuit Noise Calculations

To understanding noise figure, it is useful to consider how noise in analog circuits is modeled and applied.

Combining Noise Sources

Adding two AC voltage sources is a straightforward process using the principle of superposition. The combined voltage of two AC voltages sources, $v_1(t)$ and $v_2(t)$, is $v_{total}(t) = v_1(t) + v_2(t)$. This works because each AC voltage source is considered to be independent – that is the presence or absence of one voltage source does not influence the voltage characteristic of the other source.

However, when combining multiple noise sources, source independence needs examination. Consider two series-connected noise sources, $\overline{v_1(t)}$ and $\overline{v_2(t)}$. These represent the rms values of two noise generators. The mean-square value of these combined sources is:

$$\overline{v_{total}^2(t)} = \overline{[v_1(t) + v_2(t)]^2} \tag{3-1}$$

$$\overline{v_{total}^2(t)} = \overline{v_1^2(t)} + \overline{v_2^2(t)} + \overline{2v_1(t)v_2(t)} \tag{3-2}$$

Calculation of mean-square voltages and currents will be important in determining noise power. If the two individual noise generators are independent, then the third term in equation (3-2) has a mean-value of zero resulting in:

$$\overline{v_{total}^2(t)} = \overline{v_1^2(t)} + \overline{v_2^2(t)} \tag{3-3}$$

That is, the combined total mean-square voltage is the sum of the individual mean-square voltages of the individual sources.

Independence is achieved when combining separate devices such as two individual resistors. Lack of independence, or correlation, can occur between noise generators within an active device. When performing noise calculations, common practice is to assume independence otherwise the math quickly becomes extremely tedious.

Equivalent Active Device Noise Model

Section 2 described many of the common sources of intrinsic noise. Active devices including discrete transistors, operational amplifiers, RF amplifiers, etc. contain many separate instances of the described noise generators within the device. Separate analysis of the individual noise sources is an unwieldy exercise. For low-frequency analog amplifiers, the common practice is to combine all of these individual sources into a set of input voltage and current noise generators as shown in Figure 3.1 [4].

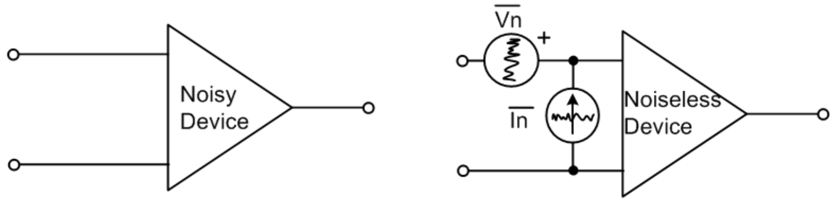

Figure 3.1 Active Device Equivalent Noise Generators

Strictly speaking, the input noise voltage and current generators have a certain amount of correlation. However, most often the error in assuming independence is small and in practice, these two noise generators are considered independent, thus rendering the noise calculation much more manageable.

When a high-impedance source is connected to the circuit, the device's noise current generator produces a large voltage across this impedance, thus dominating the total output noise of the device. Large resistance at the input also contributes a large thermal noise voltage due to large resistance value. Care must be taken when operating with large input impedances. Phase-lock loop circuits are especially sensitive to noise generated in the loop filter where it is common to have relatively large resistances in the circuit.

Circuit Noise Calculation Example

One key difference between analog circuits and RF circuits is that analog circuits use mixed impedances. Due to short wavelengths, RF circuits tend to operate more in terms of maximum power transfer, which requires homogeneous impedance between stages. Analog circuits that operate at lower frequencies are more concerned with voltages and currents than power transfer. Additionally, analog circuits can support unequal impedances between stages. Calculating noise in analog (mixed impedance) circuits uses a different procedure than RF circuits. In this section a sample analog circuit is examined for noise to demonstrate the procedure.

Figure 3.2 shows the schematic of a very simple amplifier.

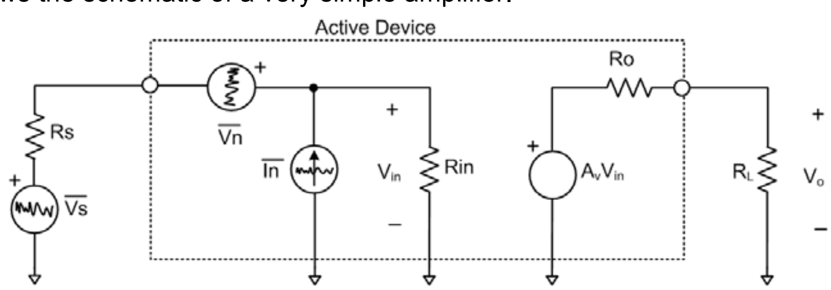

Figure 3.2 Example Analog Circuit for Noise Calculation

Even if the desired result is the noise voltage at the output, the noise analysis uses mean-square voltages. Further, it is assumed that all noise sources are independent such that the combination can be described by Equation (3-3). All resistors are considered noiseless with equivalent noise generators. In the active device, all internal noise generators, including those of Rin and Ro, have been replaced with the equivalent input noise generators as shown.

Steps in calculating output noise voltage are:

$$\overline{V_{in}^2} = \frac{\left(\overline{V_S^2} + \overline{V_n^2}\right)R_{in}^2 + \overline{I_n^2}(R_S R_{in})^2}{(R_S + R_{in})^2} \tag{3-4}$$

$$\overline{V_o^2} = \left(\frac{A_v R_L}{R_o + R_L}\right)^2 * V_{in}^2 = \left(\frac{A_v R_L}{R_o + R_L}\right)^2 * \frac{\left(\overline{V_S^2} + \overline{V_n^2}\right)R_{in}^2 + \overline{I_n^2}(R_S R_{in})^2}{(R_S + R_{in})^2} \tag{3-5}$$

$\overline{V_o^2}$ is the mean-square noise of the noise voltage at the output. Often, the rms voltage is required, for example when determining the noise on a voltage controlled oscillator tune line, in which case the rms voltage is the square root of Equation (3-5).

When the term *noise* is used with circuit analysis, the implied meaning is *noise power*. Noise power *delivered* to the load is $\frac{\overline{V_o^2}}{R_L}$. Commonly, *available noise power* is used in noise analysis. In this case the output impedance, Ro, must match the load resistance, R_L.

$$Available\ ouput\ \ noise\ power = \frac{A_v^2}{4R_o}\overline{V_{in}^2} \tag{3-6}$$

Even for this very simple example, noise calculations tend to get pretty involved. Mixed impedance, analog circuits of even modest complexity require the use of circuit simulators for noise analysis. The next section shows that for RF circuits, the noise analysis requires no more than a spreadsheet.

Equivalent Noise Bandwidth

In all the equations for the intrinsic noise generators of section 2, the bandwidth, B, is present. The term, B, represents the bandwidth of the system at the point at where the noise is measured. For instance a simplified block diagram of a receiver may appear as shown in Figure 3.3

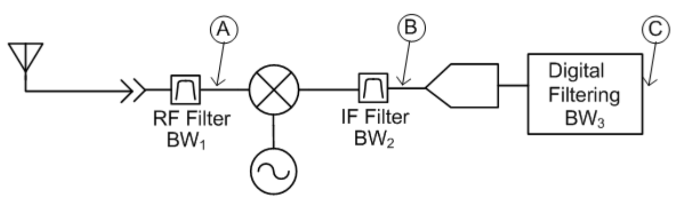

Figure 3.3 Receiver Example

At measurement point A, the system bandwidth is governed by the RF filter, BW_1. If the IF filter bandwidth is narrower than the RF filter bandwidth, then at measurement point B, the bandwidth used for noise calculation is BW_2. In systems with digital signal processing in the backend you also need to consider the bandwidth restriction as a result of the digital signal processing.

If *H(f)* is the transfer function of the filter that defines the noise power bandwidth in a system, then the mean-square value or the average power at the output of the filter is given by Equation (3-7)[5]:

$$P_{avg} = \int_{-\infty}^{\infty} |H(f)|^2 S(f) df \tag{3-7}$$

where *S(f)* is the power spectral density of the noise power in W/Hz as discussed in section 2. In words, this states that the noise power is the area under the frequency response curve of the bandwidth filter. Unfortunately the area under the frequency response curve is not represented by the 3 dB bandwidth of the filter.

The bandwidth, B, in equations for the intrinsic noise generators assumes an ideal brick-wall filter with infinitely sloped band edge skirts. Figure 3.4 shows how an ideal filter with bandwidth B compares to an actual filter:

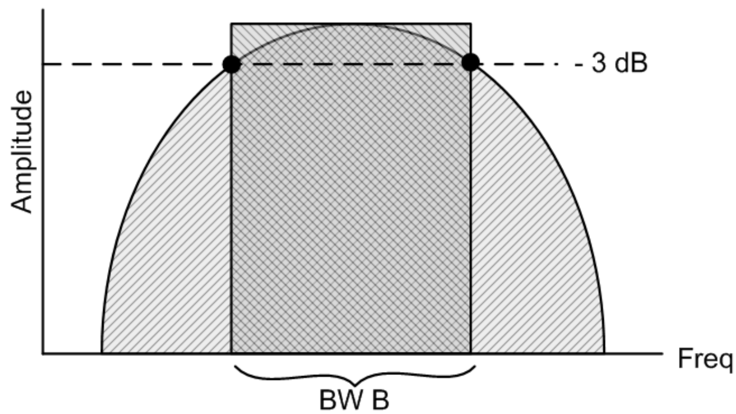

Figure 3.4 Noise Power Bandwidth

The ideal filter width is defined by the 3 dB bandwidth of the actual filter. Integrating the area under the two filter frequency response curves demonstrates that the actual filter has higher noise power than the ideal filter. Figure 3.5 shows measured noise power in a spectrum plot of white noise.

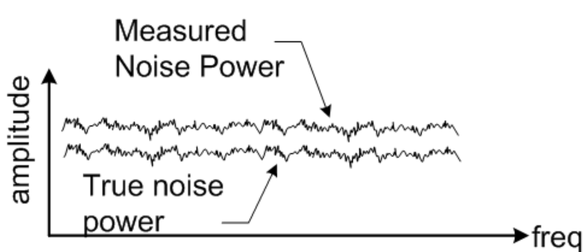

Figure 3.5 Measured versus True Noise Power

Measured noise is higher than the true average noise power level. This is because the actual filter has more area under the frequency response curve than the ideal filter, thus allowing more noise power through the actual filter.

Equivalent noise bandwidth (ENBW) is defined as the bandwidth of an ideal filter whose noise power is the same as the actual filter. ENBW is depicted in Figure 3.6.

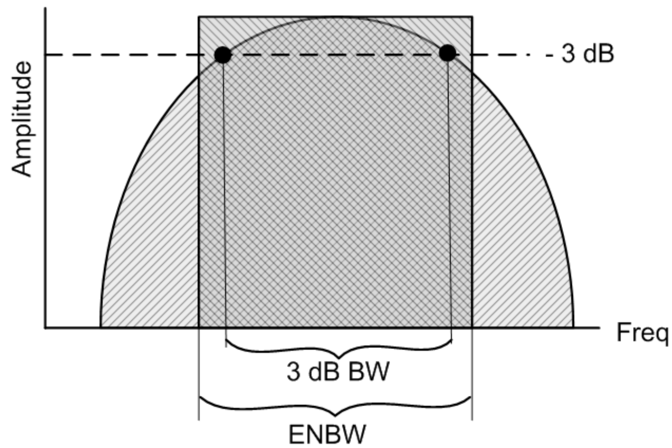

Figure 3.6 Equivalent Noise Bandwidth

Notice that ENBW is wider than the 3 dB bandwidth of the filter. To compensate for the higher average noise power of the actual filters, the ideal filter requires wider bandwidth than the 3 dB bandwidth of the actual filter. For analog filters, you must measure the frequency response of the filter to compute ENBW. For digital filters, ENBW is usually deterministic. If the digital signal processing uses windowed fast Fourier transform (FFT) to represent data in the frequency domain, then ENBW can be determined by the windowing function. Reference [6] lists ENBW for some of the more common windowing functions.

Some receivers, such as those from NI, allow the digital bandwidth to be defined by ENBW rather than 3 dB bandwidth. When selected as ENBW, the measured noise is corrected for the noise power offset. Other test and measurement receivers may have a noise marker feature that corrects for ENBW noise power offset when reporting the level of the marked signal.

4. Noise Figure Application

The focus in this section is the development of the noise figure equation. The focus is on RF circuits where the input and output impedances of the device are perfectly matched. Later this analysis expands to include circuits that posses imperfections in their port impedances.

Noise Figure Definition

Noise figure and *noise factor*, often used interchangeably in casual conversation, cannot be confused when considering the mathematics. *Noise factor* is a unit-less ratio and *noise figure* is noise factor expressed as a log relationship in decibels:

$$NF = 10log_{10}(F)\ [dB] \qquad (4\text{-}1)$$

where the term, F, is the noise factor and NF is noise figure. Noise factor is only defined for two ports of a device, even if the device, such as a frequency mixer, has more than two ports. Devices with more than two ports have noise figure defined for each combination of two ports.

Paraphrasing reference [7], noise factor between two ports of a device can be expressed as:

$$F = \frac{Total\ Output\ Noise\ Power}{Output\ Noise\ Power\ due\ to\ Input\ Noise\ Power\ Alone} \tag{4-2}$$

More formally, noise factor is expressed as: [7]

$$F = \frac{N_O}{N_i G_A} \tag{4-3}$$

where N_o is the available noise power at the output of the device, N_i is the available thermal noise power of the source resistor at the input of the device and G_A is the so-called available gain of the device. Input noise power, Ni, has been defined by equation (2-3) to be kT_oB, where T_o is defined by IEEE to be 290 K. The descriptor, *available*, used in all of the terms of the noise factor equation in (4-3) refers to maximum power transfer as presented in Figure 2.5. When all the impedances of the system, including the device input/output impedance, source impedance and output impedance, are matched to the characteristic impedance of the system (normally 50 Ω) all powers are *available powers*. Equations for noise figure are not limited to matched-impedance systems [8]. This section first develops the analysis using matched impedances and later expands on this analysis with mixed-impedance system blocks.

Equation (4-3) is the formal IEEE definition of noise factor; however, this equation can be manipulated by realizing the available gain can be expressed as:

$$G_A = \frac{S_O}{S_i} \tag{4-4}$$

where S_o is the available signal power at the output (under conditions that the output impedance of the device matches the load impedance) and S_i is the available signal power from the input source. Then noise factor can be expressed as:

$$F = \frac{S_i / N_i}{S_O / N_O} = \frac{Input\ SNR}{Output\ SNR} \tag{4-5}$$

SNR is signal-to-noise ratio. Equation (4-5) gives the intuitive sense that noise factor is the degradation in SNR of a circuit block. If the circuit block has a noise figure of 5 dB and the input noise power of that block is kT_oB, then the SNR at the output of that block is 5 dB less than the input SNR.

Let N_D be the device-added noise referred to the input of the device. Output noise power then becomes: $N_o = G_A(N_i + N_D)$. Now, noise factor can be expressed as:

$$F = \frac{G_A(N_i + N_D)}{N_i G_A} = 1 + \frac{N_D}{N_i} = 1 + \frac{N_D}{kT_oB} \tag{4-6}$$

When the noise factor of a device is known, the device-added noise can be calculated from (4-6) as:

$$N_D = (F-1)kT_oB \tag{4-7}$$

Figure 4.1 shows a graphical representation of the terms involved in the noise factor equation.

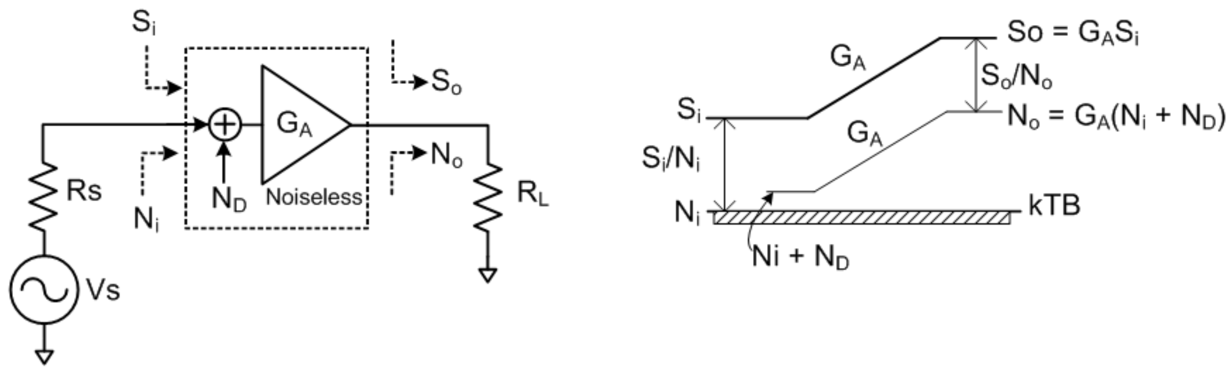

Figure 4.1 Graphical View of Noise Factor

Device-added noise, N_D, is summed at the device's input allowing the device to be considered noiseless. Treating device-added noise in this manner simplifies the calculation of system noise. Input SNR is defined as the SNR at the input of the noisy device. Device-added noise combines with input noise and then both signal and combined noises experience the same available gain, G_A, through the device. As shown, output SNR is less than input SNR as a result of device-added noise.

Attenuator Noise Figure

For active devices such as amplifiers, noise figure is normally specified by the manufacturer. Lossy, passive elements such as attenuators, filters, PC board traces, and so on do not normally have noise figure specified. Noise figure of passive, lossy elements is the loss of that element. For instance, a 10 dB fixed attenuator has a 10 dB noise figure. Figure 4.2 sheds some light on calculating the noise figure of a loss element.

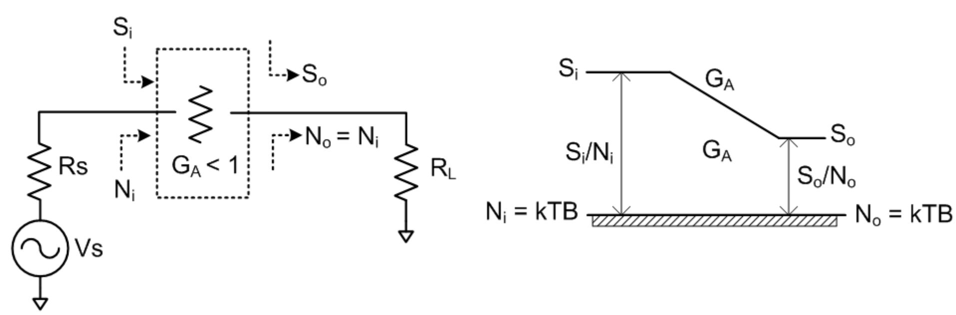

Figure 4.2 Attenuator Noise Figure

Input noise, when calculating noise figure, is by definition kT_oB. The loss element generates thermal noise power. When the output impedance of the loss element is matched to the load impedance, the output available noise power is also kT_oB. The input signal, however, experiences a loss transitioning through the passive device. Noise factor for a loss element then becomes:

$$F = \frac{S_i/_{N_i}}{S_o/_{N_o}} = \frac{S_i/_{kToB}}{S_o/_{kToB}} = \frac{1}{G_A} \quad (4\text{-}8)$$

Available gain for a loss device is less than one rendering noise factor greater than 1 and noise figure greater than 0 dB.

General Output Noise Calculation

Noise figure is calculated with the input noise power set to kT_oB by definition. When the input noise exceeds kT_oB which can occur for downstream stages in a system of cascaded circuit elements, the task at hand shifts from calculating noise figure to calculating noise power level at the output of each stage. Figure 4.3 illustrates how to compute output noise when $N_i > kT_oB$.

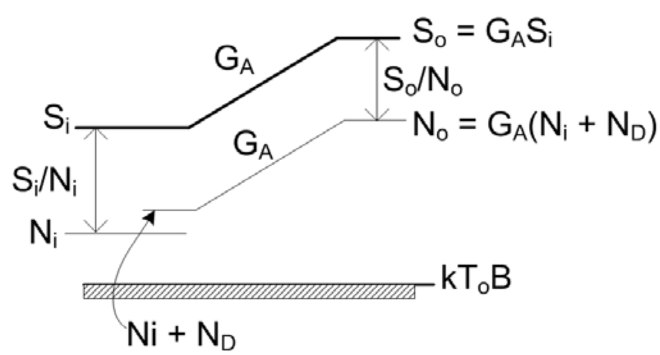

Figure 4.3 Amplifier Noise Calculation with N_i > kTB.

In these cases, the device noise figure is either specified by the manufacturer, as in the case of active devices, or can be computed, as in the case of passive structures. From the known device noise figure, the device-added noise, N_D, can be computed using Equation (4-7). The available output noise power then becomes:

$$N_o = G_A(N_i + N_D) = G_A(N_i + kT_oB(F-1)) \quad (4\text{-}9)$$

For a passive device, the available output noise power uses the same equation as (4-9) with one important caveat. Earlier it was shown that when the device is output matched to the load impedance, the device generates a minimum available output noise power of kT_oB. So if computed output noise power using Equation (4-9) is less than kT_oB, a minimum value of kT_oB must be imposed on Equation (4-9). Cascaded noise where input noise is greater than kTB is depicted in Figure 4.4

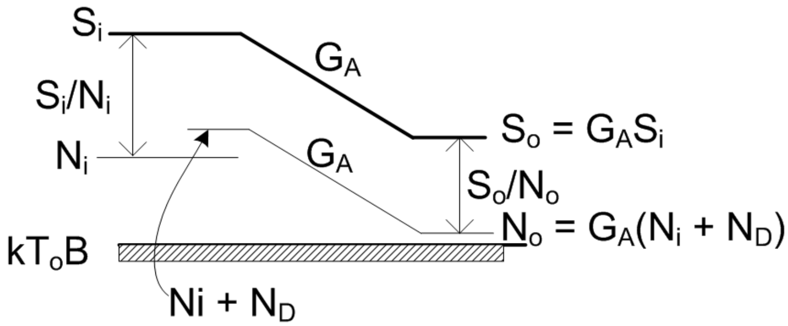

Figure 4.4 Passive Device Output Noise Power with N_i > kTB.

System Noise Calculations

Cascading multiple blocks in a system to compute either output noise power or system noise figure is illustrated using Figure 4.5

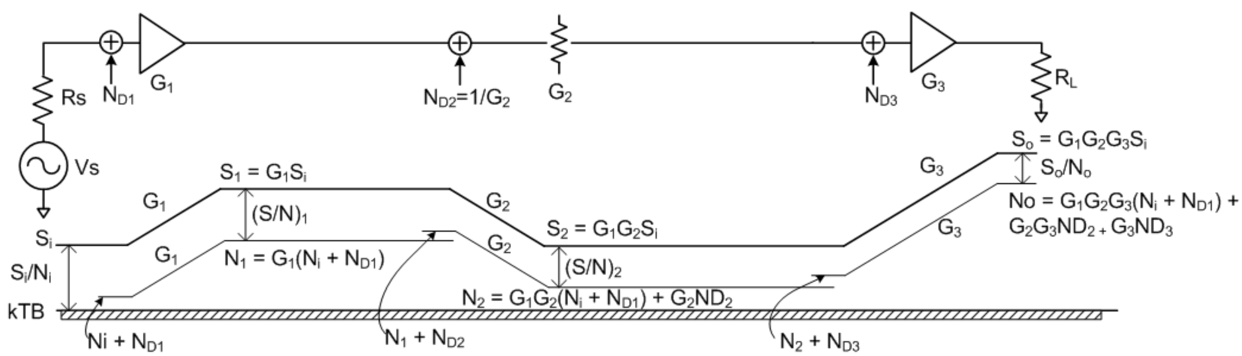

Figure 4.5 Cascaded Noise

Calculation progresses one stage at a time from input to output. At the output of any given stage, noise power is computed using Equation (4-9). Signal power for each stage can also be computed if desired. Progressing to the next stage, the input noise power of that stage is the output noise power of the previous stage. Final system noise figure can be computed using equation (4-8).

Friis [8] shows that the noise factor of a cascaded system is given by:

$$F_T = F_1 + \frac{F_2 - 1}{G_1} + \frac{F_3 - 1}{G_1G_2} + \dots \qquad (4-10)$$

This equation reveals the effectiveness of adding a preamplifier to the system. By using a high gain amplifier as the first stage, gain G_1, which appears in the denominator of all but the first term, tends to make all subsequent terms insignificant compared with the first term. So, the total system noise factor, F_T, is approximated by the first gain stage's noise factor, F_1.

Appendix A reviews the use of signal flow graphs in the design of cascaded RF systems. Appendix B builds on the information in Appendix A to help you understand the equations for available power gain and transducer power gain. This information can assist in determining the error in the system noise figure using Equation (4-10) when the individual stages are not designed for available power gain.

Optimum Input Noise Match

Noise figure specifications for discrete components are often listed as *minimum noise figure*, NF_{min}. To achieve NF_{min}, an optimum impedance must be presented to the input of the device. In Figure 4.6, noise circles plotted on the Smith chart are used to determine the noise figure as a function of the reflection coefficient looking back from the input port of the device, Γ_S.

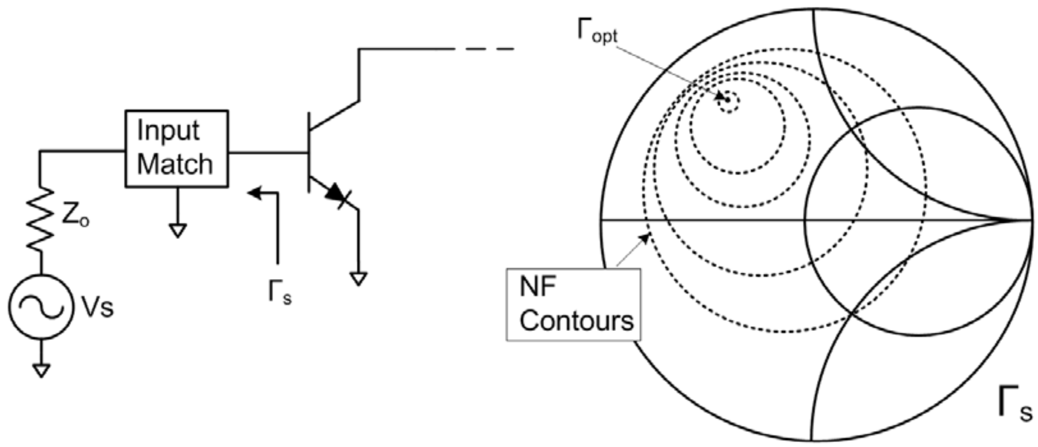

Figure 4.6 Optimum Noise Match

The optimum impedance match for minimum noise figure is represented by reflection coefficient Γ_{OPT}. Each dotted line circle represents contours of constant noise figure which enables the designer to determine the noise figure when the input impedance strays away from the optimum. Parameters to generate the noise circles in some cases are sometimes given by the device manufacturer; RF simulation software can then generate these noise circles.

The design approach appropriate for narrow band applications is to construct an input matching network using reactive, non-lossy components. This network transforms the system characteristic impedance to a desired noise match at the input of the device. Consult reference [11] for more information on designing impedance matching circuits for RF devices.

Frequency Translating Device Noise Figure

Frequency translating devices, such as mixers, have the potential to convert noise from several frequencies across the spectrum as shown in Figure 4.7.

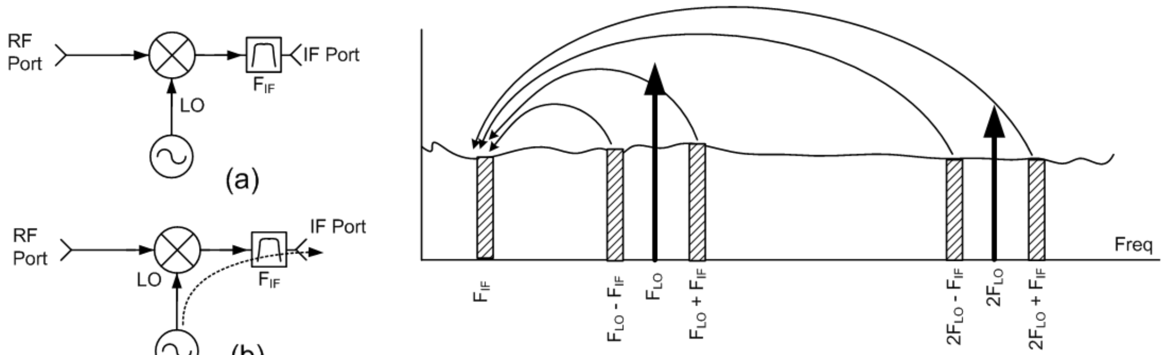

Figure 4.7 Noise Figure of a Frequency Translating Device

In this example, a mixer is configured as a downconverter with a fixed IF frequency. Banded noise separated by +/- F_{IF} from any of the Local Oscillator (LO) harmonics can frequency translate down to the final IF. Figure 4.7 (b) shows an additional source of noise which is noise on the LO at the IF frequency leaking past the mixer and appearing directly at the IF.

Reference [7] states that noise figure is defined for input noise that appears at the output from the "principle-frequency transformation of the system". The implication is that noise from one source of frequency translation should be considered in the calculation of noise figure. For example, if the system is designed to be calibrated for F_{LO} + F_{IF}, then banded noise from all other frequencies in the spectrum should not be considered. The terminology used to describe this is *single-sideband* (SSB) noise figure.

Care in the measurement of mixer noise figure must be considered to ensure SSB noise figure. Filtering at the RF and LO ports is one possible consideration. For passive mixers, a first order approximation is to consider the SSB noise figure as being the same value as the conversion loss of the mixer.

5. Y-Factor Noise Figure Measurement Technique

Up to this point, sources of noise, concept of noise figure, and system noise analysis have been presented. The focus of this section now shifts to the measurement of noise figure including the actual measurement procedures and more importantly, the associated measurement uncertainties. The first noise figure technique discussed is the so called Y-factor technique.

The Y-factor technique uses an *excess noise source* (ENS) to provide two levels of calibrated noise power at the input of the device under test (DUT). Figure 5.1 shows the measurement setup for the Y-factor technique:

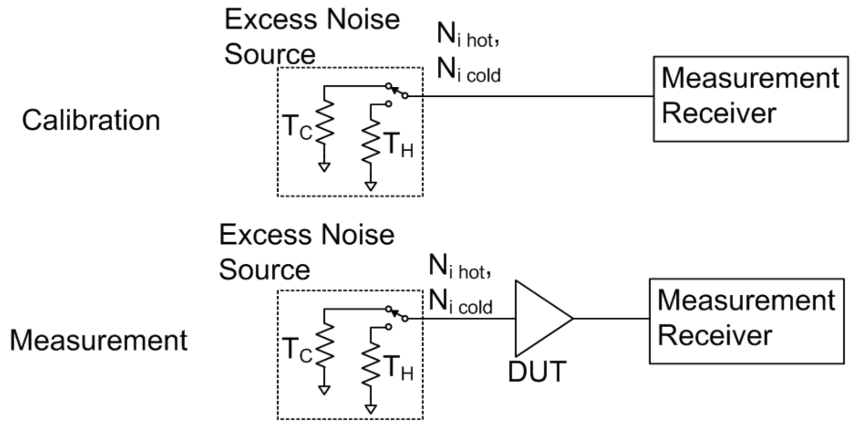

Figure 5.1 Y-Factor Measurement Setup

Two steps are required in this measurement procedure: 1) *calibration* where the ENS is connected to the measurement receiver and 2) *measurement* where the DUT is inserted between the ENS and the measurement receiver.

The ENS uses an avalanche diode to generate broadband, spectrally flat noise. When the diode is biased on, the relatively high noise power is given as $N_H = kT_HB$. This is available noise power, from Equation (2-3), with a 'hot' noise temperature. When the diode is biased off, the relatively low noise power is given as $N_C = kT_CB$. This is available noise power with a 'cold' noise temperature.

Consider noise measured at the output of the DUT, including both the input noise the noise contribution of the measurement receiver. With the ENS in its 'on' (hot) state, the DUT output noise is given by:

$$N_{O\,hot} = GN_{i\,hot} + GN_D = kBG[T_H + T_O(F-1)] \tag{5-1}$$

With the excess noise source in its 'off' (cold) state, the DUT output noise is given by:

$$N_{O\,cold} = GN_{i\,cold} + GN_D = kBG[T_C + T_O(F-1)] \tag{5-2}$$

The parameter, Y, by definition, is the ratio of noise with the ENS "on" to noise with ENS "off". Taking the ratio of Equations (5-1) to (5-2) results in the parameter Y:

$$Y = \frac{N_{o\,hot}}{N_{o\,cold}} = \frac{T_H + T_O(F-1)}{T_C + T_O(F-1)} \tag{5-3}$$

Re-arranging terms:

$$F = \frac{\frac{T_H - T_o}{T_o} - Y\frac{T_C - T_O}{T_O}}{Y - 1} \tag{5-4}$$

T_C is the ambient temperature of the excess noise source and T_O is by definition 290 K. T_H can be determined from the ENS calibration data (discussed below).

Equations (5-3) and (5-4) demonstrate an inherent advantage of the Y-factor measurement method: this method relies on the ratio of measurements. Items in the measurement receiver such as absolute amplitude accuracy and equivalent noise power bandwidth are common to both the hot and cold noise measurements. The parameter Y is a ratio of these two noise powers where these common error terms cancel.

The ENS is characterized with what is termed the *excess noise ratio* (ENR). This value, which is device and frequency dependent, is data normally provided by the ENS manufacturer. One common misperception is that ENR is the ratio of noise with the noise source “on” to noise with noise source “off”. ENR is actually defined according to Equation (5-5):

$$ENR\ [dB] = 10log_{10}\left(\frac{T_H - T_C}{T_O}\right) \qquad (5-5)$$

Hot temperature T_H can then be extracted from Equation (5-5):

$$T_H = T_C + T_O * 10^{ENR/10} \qquad (5-6)$$

The measurement of ENR stems from metrology grade measurements of noise powers when the noise source is “off”, corresponding to “cold” noise and when the noise source is “on”, corresponding to “hot” noise. The “cold” and “hot” noise temperatures are computed by extraction from Equation (2-3): T = Ni/kB. These temperature values are then applied to Equation (5-5) to arrive at a value for ENR.

ENR is defined so the cold temperature is T_o, or 290 K. When the physical temperature during the DUT measurement process differs from 290 deg K, a slight correction in the ENR value can be computed by adding $[T_O – T_C] / T_O$ to the calibrated linear ENR value:

$$Corrected\ ENR\ [dB] = 10log_{10}\left[10^{ENR/10} + \frac{T_o - T_c}{T_o}\right] \qquad (5-7)$$

This correction is quite negligible at room temperature; for instance if T_C = 25 °C the correction is -0.004 dB. Even at T_C = °deg C, the correction is only -0.018 dB

To compute the noise figure of the DUT, Equation (4-10) must be manipulated resulting in Equation (5-8):

$$F_{DUT} = F_{meas} - \frac{F_{cal} - 1}{G_{DUT}} \qquad (5-8)$$

F_{cal} is calculated using Equation (5-4) when the ENS is connected to the measurement receiver in Figure 5.1. F_{meas} is the total system noise factor when the DUT is inserted in between the ENS and the measurement receiver. Equation (5-8) removes the measurement receiver’s noise factor contribution from the total system noise factor.

The procedure requires four noise measurements: hot/cold using the calibration setup and hot/cold using the measurement setup. DUT Gain, G_{DUT}, can be calculated from the four noise measurements.

$$N_{meas\ hot} = GN_{i\ hot} + GN_{D\_DUT}$$

$$N_{meas\ cold} = GN_{i\ cold} + GN_{D\_DUT}$$

$$N_{cal\ hot} = GN_{i\ hot} + GN_{D\_DUT} + N_{D\_Rcvr}$$

$$N_{cal\ cold} = GN_{i\ cold} + GN_{D\_DUT} + N_{D\_Rcvr}$$

$$G_{DUT} = G = \frac{N_{meas\ hot} - N_{meas\ cold}}{N_{cal\ hot} - N_{cal\ cold}} \qquad (5-9)$$

N_{D_DUT} and N_{D_Rcvr} are the DUT and measurement receiver device-added noises. With G_{DUT} calculated, all the terms in Equation (5-8) are known so that the DUT's noise factor, F_{DUT}, can be calculated. DUT noise figure is given by $NF_{DUT} = 10\log_{10}(F_{DUT})$.

This section assumes matched impedances of all elements in the measurement chain: ENS, DUT, and the measurement receiver. Section 6 analyzes the uncertainties considering mismatch error.

6. Minimizing Y-Factor Measurement Uncertainty

Making accurate noise figure measurements requires a certain level of care. This section describes some best practices that can help you avoid some common pitfalls in the measuring noise figure. In addition, measurement accuracies stemming from impedance mismatches and measurement receiver noise floor are discussed.

Shielding

An often overlooked problem during the noise figure measurement procedure is over-the-air signals impinging on the DUT.

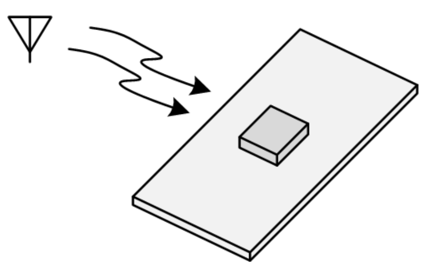

Figure 6.1 Interference during Noise Figure Measurement

The issue of the DUT picking up extraneous over-the-air signals is especially prevalent when measuring high gain DUTs that operate in some of the common communications channels (900 MHz, 1.8 GHz, 2.4 GHz, etc.).

The solution is to create a Faraday cage around the DUT to eliminate interference from outside sources. A fully shielded enclosure incorporating bulkhead RF connectors is warranted:

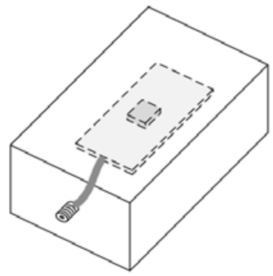

Figure 6.2 Shield Enclosure

Power Supply Filtering

Noise on power supply lines, especially if switching power supply technology is used, can interfere with the noise figure measurements. If the goal is to isolate the noise figure measurement from other extraneous sources of noise, extra filtering on the power supply lines to the DUT may be required.

If the DUT is embedded on a circuit with other sources of noise, such as digital clocks, some care is needed to ensure that the noise figure measurements are not made at the clock frequencies or provide some level of isolation between the DUT and other interfering noise generators in the system.

DUT and Measurement Receiver Spurs

Spurious signal either from the DUT or the measurement receiver, may interfere with the noise figure measurement. Figure 6.3 demonstrates how a low-level discrete tone can show up as a bump in the frequency spectrum.

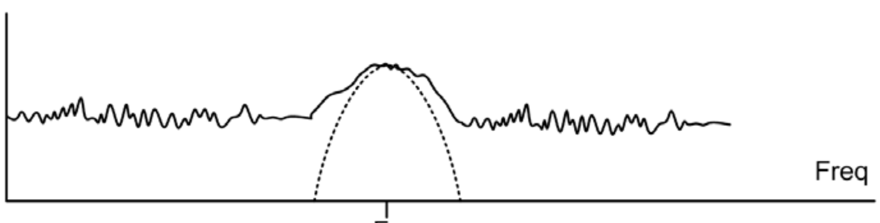

Figure 6.3 Measurement Spurs

The discrete tone convolves with the frequency response of the measurement receiver's resolution bandwidth (RBW) filter. This is a frequency domain convolution process. The result is a broadening in the range of frequencies where the spurious tone affects the noise floor.

Noise figure measurements are made at very low amplitudes. Spurious signals that are normally low enough to not interfere with other common measurements could become a problem with noise measurements. You should also avoid cardinal frequencies that are prone to spurious signal energy. Multiples of 10 MHz in common test measurement receivers are examples of cardinal frequencies to avoid.

Adjusting the measurement frequency away from the spur is one possible idea to avoid the spur. The frequency must be adjusted more than the measurement bandwidth of the measurement receiver.

Reducing the measurement bandwidth can be used if there is suspicion that the DUT's noise figure at the new frequency would not reflect the noise figure value at the original desired frequency.

To speed up measurements, the measurement receiver is often set to zero span, centered at the frequency of interest. Zero span yields an amplitude versus time measurement. If the spur is within the RBW filter range, deciphering whether or not a spur is present is especially difficult. One should view the spectrum at the measurement frequency of interest to ensure no spurious signals are present before engaging the zero span measurement setting.

The noise figure measurement application software NI offers includes a spur recognition routine to alert the user of potential spurs before making the noise figure measurement.

Impedance Mismatch Uncertainty Considerations

Impedance mismatch is one of the larger uncertainties in making a successful noise figure measurement. As shown in Figure 6.4(a), the voltage transmitted to the load is not necessarily the voltage incident upon the load.

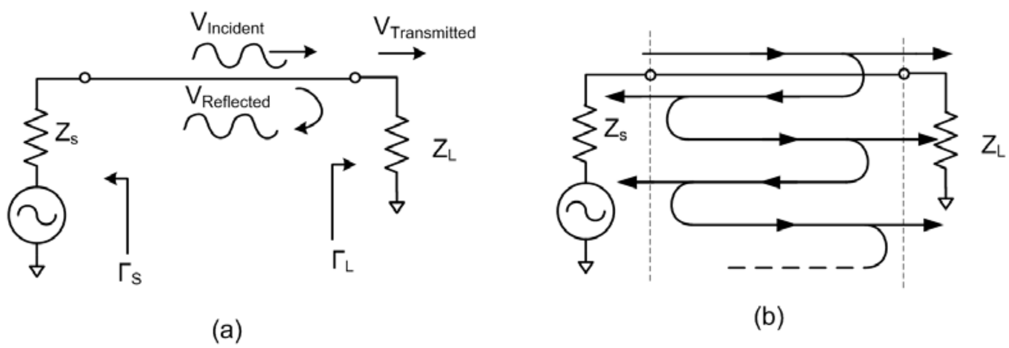

Figure 6.4 Signal Reflections Due to Source/Load Impedance Mismatch

A portion of the incident voltage reflects back to the source. The reflected voltage's value depends on the load impedance:

$$V_{Reflected} = \Gamma_L V_{Incident} \qquad (6-1)$$

where Γ_L is the load's reflection coefficient. If the load impedance is given in terms of return loss, then

$$\Gamma_L = 10^{\left(-Return\ Loss\ [dB]/_{20}\right)}$$

Equation (6-1) is in terms of the incident and reflected voltages at the load interface. Figure 6.1 (b) shows that the reflected voltage will re-reflect at the source interface. This re-reflected voltage then reflects once again at the load interface. This re-reflection process continues indefinitely. The total transmitted voltage is a vector combination of the series of re-reflected signals at the load interface.

Analyzing the power transmitted to the load using signal flow graphs as outlined in Appendix A is one established technique. The signal flow graph for the simple system in Figure 6.4 is shown in Figure 6.5:

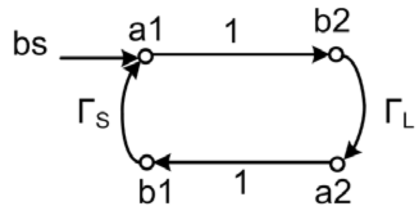

Figure 6.5 Source/Load Signal Flow Graph

Following the theory presented in Appendix A, the power transmitted to the load is:

$$P_L = |b_2|^2 - |a_2|^2 = |b_2|^2(1 - |\Gamma_L|^2) \qquad (6-2)$$

$$P_L = \frac{1-|\Gamma_L|^2}{|1-\Gamma_S\Gamma_L|^2} \qquad (6-3)$$

The numerator in Equation(6-3) represents a power loss and the denominator represents an uncertainty in the power delivered to the load. For worst case analysis where the phases of the reflection coefficients are unknown, Equation (6-3) can be expressed as Equation (6-4):

$$P_L = \frac{1-|\Gamma_L|^2}{(1 \pm |\Gamma_S||\Gamma_L|)^2} \qquad (6-4)$$

For the Y-factor noise figure measurement technique, the mismatch uncertainty can occur during the calibration step as well as the measurement portion. Three mismatch interface planes are depicted in Figure 6.6:

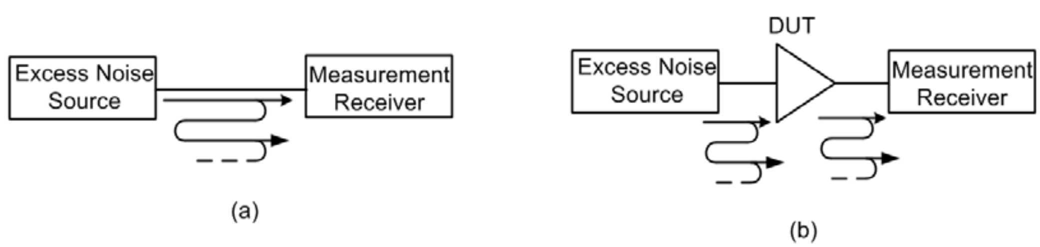

Figure 6.6 Impedance Mismatch Effects in Y-Factor Measurement

When the DUT's reverse isolation is sufficiently large, the mismatch uncertainties at the DUT input and output of Figure 6.6 (b) can be treated independently using Equation (6-3) if phases are known or Equation (6-4) if only magnitudes of the reflection coefficients are known. For the general case where input and output port independence cannot be guaranteed, then the equations in Appendix A need to be employed.

Section 9 outlines a procedure for modeling the entire noise figure measurement uncertainty calculations. Figure 6.7 shows the uncertainty in making a Y-factor noise figure measurement considering only impedance mismatches using this modeling procedure.

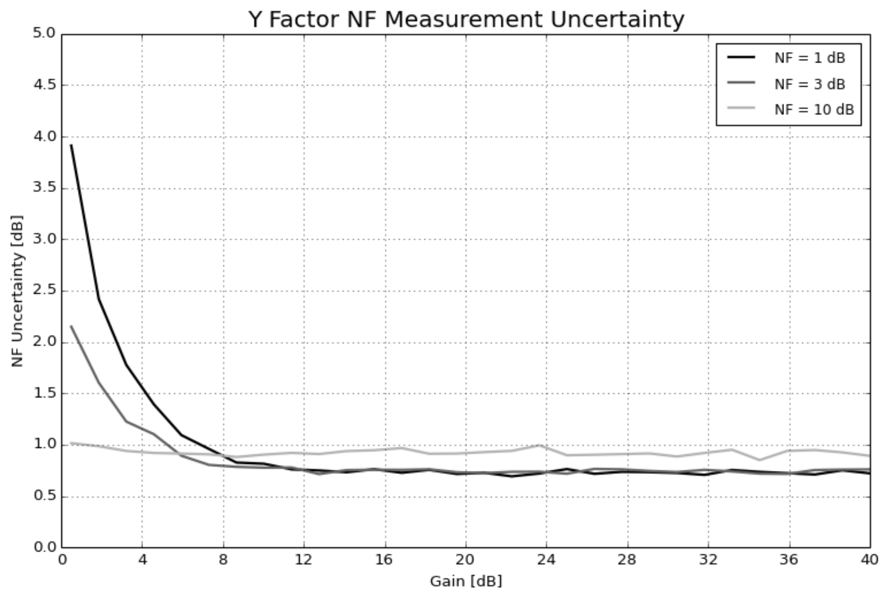

Figure 6.7 Noise Figure Measurement Uncertainty Due to Impedance Mismatch

Uncertainty is considered as the mean error +/- two standard deviations from a noise figure measurement distribution using multiple measurements according to a Monte Carlo analysis technique. The phases of the DUT, ENS and measurement receiver are randomly distributed. For each combination of port phases in the population, a noise figure computation is made.

A noticeable trait in Figure 6.7 is the measurement uncertainty increases for lower gain, lower noise figure DUTs. As the DUT's noise figure increases, overall measurement uncertainty increases for all values of DUT gain.

Impedance mismatch is particularly bothersome in that it affects the Y-factor measurement in two ways. First, the calculation of the value Y in Equation (5-3) is corrupted. Secondly, DUT gain in Equation (5-9) is affected. The cascaded noise figure in Equation (4-10) depends on the calculated gain being available gain where the output load is conjugately matched to the DUT's output. When conjugate matching is not possible, the calculated gain approximates *operating power gain* as defined in Appendix B. The term *insertion gain* has been coined to describe the gain measured as part of the Y-factor technique. The uncertainty calculations outlined in Section 9 do in fact use the insertion gain; this gain is a natural outcome of the gain as described by Equation (5-9). Substituting measured power gain for available power gain leads to additional DUT noise figure measurement uncertainty when using Equation (5-8).

Receiver Noise Figure

When coupled with a mismatch between the DUT's output impedance and the measurement receiver's input impedance, the receiver's noise figure can have a dramatic impact on measurement accuracy. Figure 6.8 shows the high sensitivity of the noise figure measurement uncertainty as a function of the receiver noise figure. The x-axis is the DUT gain, the y-axis is the noise figure measurement uncertainty and each trace represents the receiver noise figure.

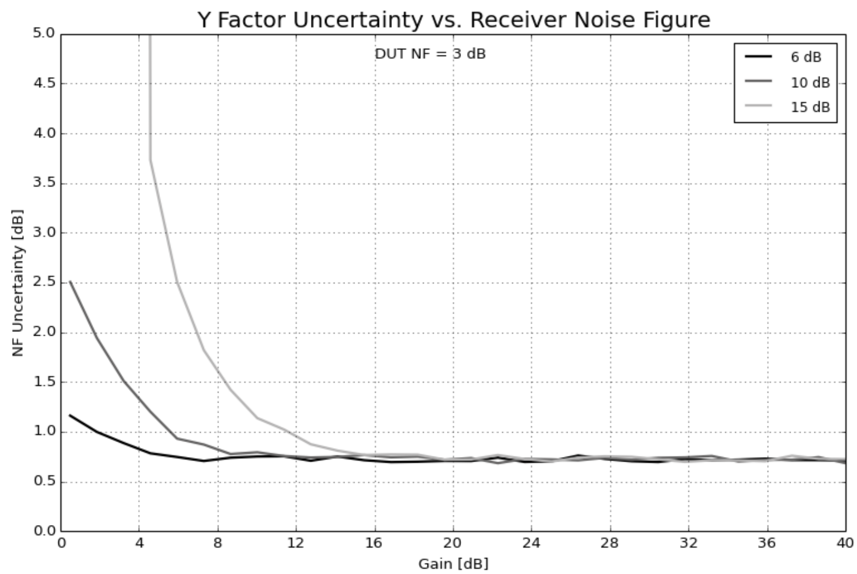

Figure 6.8 Impact of Measurement Receiver Noise Figure on NF Measurement Accuracy

Common practice is to include a low-noise, high-gain preamplifier at the input of the measurement receiver to reduce the effective noise figure of the combined preamp/measurement receiver subsystem.

Input and Output Fixed Attenuators

Adding a fixed attenuator (pad) in series with a load effectively improves the overall impedance match of the system. Figure 6.9 helps to illustrate how fixed attenuators improve the effective return loss of a poorly matched device when the attenuator is placed in series with the device:

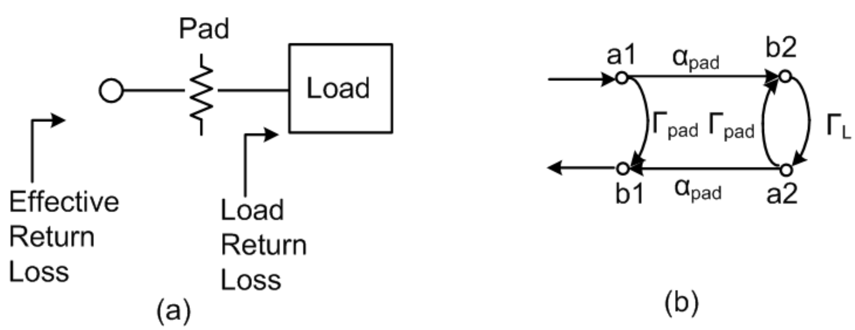

Figure 6.9 Fixed Attenuator Added to a Load

To a first order approximation, if the load has a certain return loss expressed in dB, then the effective return loss at the pad interface is:

Effective Return Loss [dB] = 2xPad Attenuation [dB] + Load Return Loss [dB]

Adding a 3 dB pad to a load with 10 dB return loss can improve the effective return loss to be 16 dB.

The actual effective impedance calculation is a bit more involved, requiring signal flow graph analysis using the signal flow graph of Figure 6.9 (b). The effective reflection coefficient is:

$$\Gamma_{effective} = \Gamma_{pad} + \frac{\alpha_{pad}^2\,\Gamma_L}{1 - \Gamma_{pad}\Gamma_L} \qquad (6-5)$$

where α_{pad} is the linear s21 gain of the pad. Equation (6-5) shows that the effective return loss cannot be any better than the return loss of the pad itself, revealing the necessity of using a high quality fixed attenuator.

When including fixed attenuators in the Y-factor noise figure measurement, the calibration planes are defined as shown in Figure 6.10.

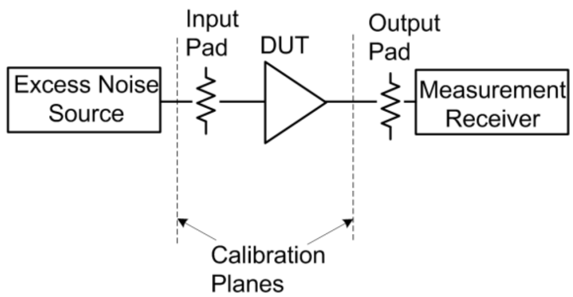

Figure 6.10 Calibration Planes When Fixed Attenuators Are Added to the Measurement System

During the calibration portion of the noise figure measurement, the ENS is connected to the combined output pad/measurement receiver combination. The input pad is not part of the calibration procedure. Figure 6.11 shows the cascaded model of the noise figure system when input and output pads are included.

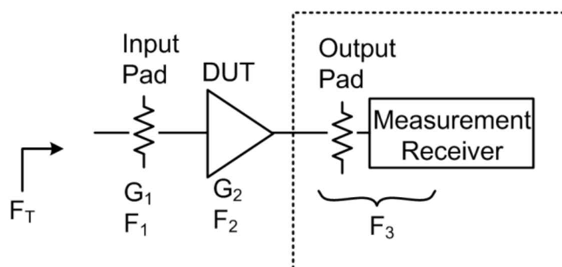

Figure 6.11 Input and Output Pads Applied to the Y-Factor Method

The noise figure of the measurement system is increased by the output pad value, yielding a noise factor of F_3. Gain, G_1G_2 is the combined gain of the input pad and the DUT. During the calibration process, F_3 is calculated using equations (5-3) and (5-4). F_T is calculated during the measurement portion. G_1G_2 is a measured value and is calculated using Equation (5-8). G_1 and F_1 associated with the input pad are known values. Now, the DUT noise factor, F_2 can be extracted from:

$$F_T = F_1 + \frac{F_2 - 1}{G_1} + \frac{F_3 - 1}{G_1G_2} \qquad (6-6)$$

$$F_2 = G_1\left[F_T - F_1 - \frac{F_3 - 1}{G_1 G_2}\right] + 1 \qquad (6-7)$$

Figure 6.12 shows the effects on Y-factor noise figure measurement uncertainty using input and output pads. Clearly there is a demonstrated improvement in measurement uncertainty when adding an input pad to a DUT with poor input return loss. However, precaution is warranted when using an output pad. The output mismatch uncertainty is improved, however the degraded effective noise figure of the measurement receiver due to the addition of the output pad has an adverse effect on measurement uncertainty as demonstrated by Figure 6.12.

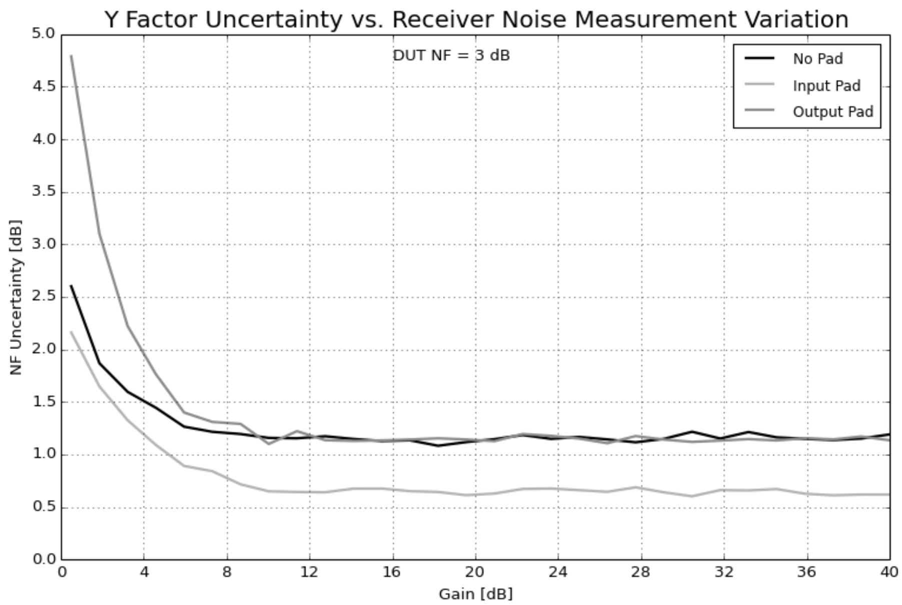

Figure 6.12 NF Uncertainty with Input and Output Pads

Receiver Noise Measurement Variation

Sometimes referred to as display jitter, receiver noise measurement variation is a potentially large variance in the measurement of noise in the measurement receiver. Trace averaging is required to reduce the variance in the noise measurement. Figure 6.13 demonstrates the effect of trace averaging within the measurement receiver on the measurement of noise.

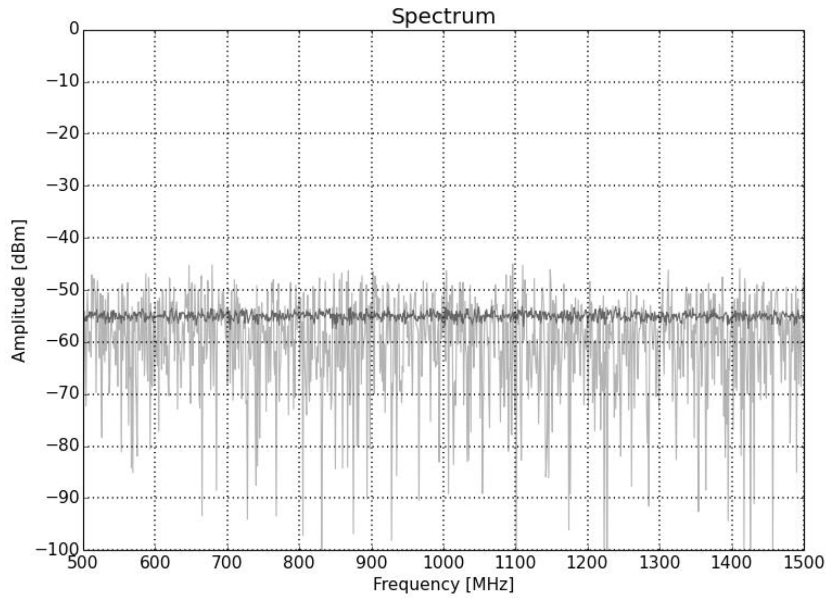

Figure 6.13 Noise Measurement Variation versus Trace Averaging

The lighter trace shows the spectrum of a noise measurement with no trace averaging employed whereas the darker line is the same measurement with 100 trace averages. Note the dramatic improvement in the variance of the noise measurement with trace averaging. Mathematically the variance of noise measured on a linear scale decreases by a factor 1/N, with N being the number of trace averages [12]:

$$\sigma_{average}^{2} = \frac{\sigma^{2}}{N} \qquad (6-8)$$

There is a diminishing return on variance improvement as a function of the number of averaging samples. Measurement time scales linearly with the number of averaging samples, but the variance improvement scales with a 1/N, nonlinear function.

The National Instruments noise figure measurement software uses a zero span setting for the measurement of the noise. That is, the measurement receiver is tuned to the desired measurement frequency and measures noise only at that frequency (no frequency sweeping involved). This is effectively a time domain measurement of noise. Averaging is performed by summing the linear scale amplitudes of the time domain trace samples and dividing by the number of time domain samples. The longer the data acquisition, the more data samples and hence, the greater the variance improvement.

NI noise figure measurement software includes three measurement accuracy settings: Speed setting uses a 5 msec data acquisition time interval yielding a standard deviation in the noise measurement of 0.22 dB. Accuracy setting (default) uses a 50 msec data acquisition time interval yielding a 0.07 dB noise measurement standard deviation. Finally, the Enhanced Accuracy setting uses a 200 msec data acquisition time interval yielding a 0.03 dB noise measurement standard deviation.

Figure 6.14 shows the noise figure measurement uncertainty as a function of the standard deviation of the measurement variation.

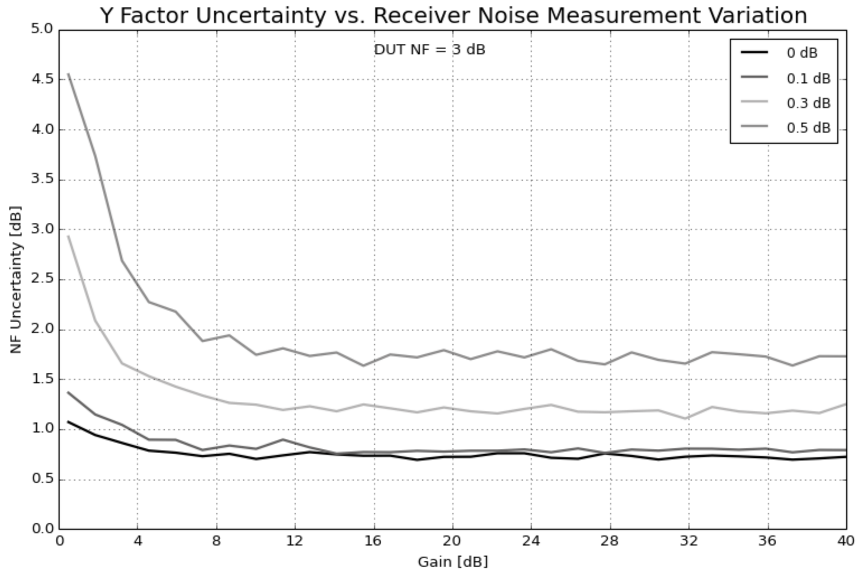

Figure 6.14 Noise Figure Measurement Uncertainty versus Receiver Measurement Variation

The trace labeled "0 dB" is a simulation with no noise measurement variation (that is, perfect noise measurement). The other traces refer to the empirically determined standard deviations in the noise measurement variation. The measurement uncertainty degrades more strongly for lower gain DUTs, however, as the gain increases the uncertainty floor is largely independent of DUT gain.

DUT Noise Figure Dependence on Source Match

Another source of noise figure measurement error stems from the DUT's noise figure dependence on the impedance presented to the input of the device. This idea was presented in Figure 4.6 during the discussion of the optimum input noise match. Since the Y-factor technique uses an ENS with nominally 50 Ω impedance, achieving minimum DUT noise figure is quite unlikely. Some means of impedance transformation is required to achieve optimum DUT noise match.

One technique to establish a desired source impedance to the DUT is to use an impedance tuner as depicted in Figure 6.15.

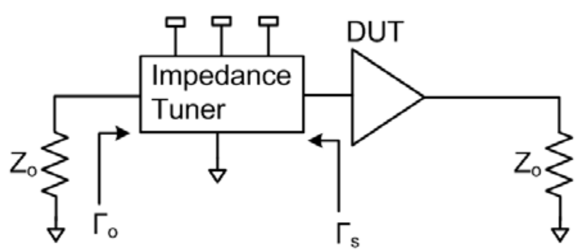

Figure 6.15 Source Pull Measurement Technique

Mechanical and electronic load tuners are available to create the desired source reflection coefficient, Γ_S, presented to the DUT input. Γo is the reflection coefficient associated with the characteristic impedance of the system, Zo.

Another technique is to design the input matching circuit using techniques outlined in reference [11]. Then consider this matching network as part of the DUT as shown in Figure 6.16.

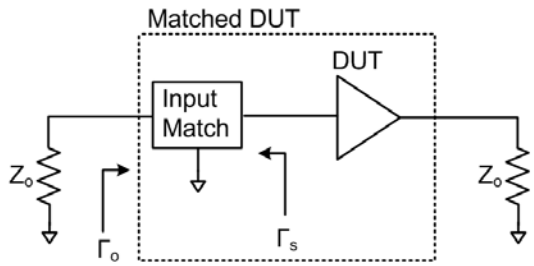

Figure 6.16 Incorporating Input Matching as Part of the DUT

The idea is to use passive, lossless components to present a nominal impedance of Z_o looking into the overall matched DUT and to present an optimum noise impedance looking backwards from the DUT input. Γo and Γs are the input and output reflection coefficients associated with the system characteristic impedance Zo and the optimum impedance as seen by the DUT.

Excess Noise Source On/Off Impedance Change

The impedance of the ENS can differ between its "on" and "off" states. This is usually specified as a reflection coefficient on/off ratio: $\Gamma_{on/off}$. These values are typically on the order of 0.01. Figure 6.17 shows Y-factor measurement uncertainty with various levels of $\Gamma_{on/off}$ ratios.

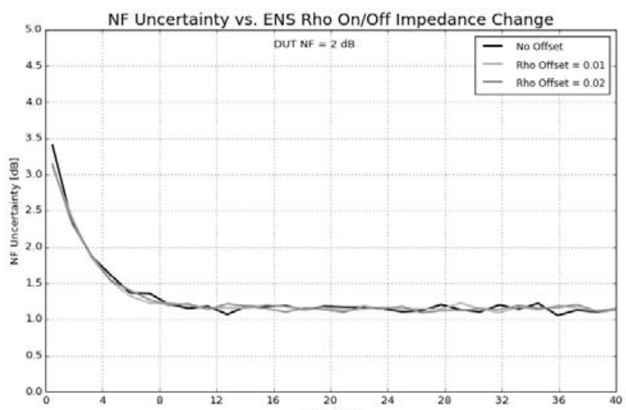

Figure 6.17 Noise Figure Uncertainty versus ENS Reflection Coefficient On/Off Change

The curve labeled "No Offset" represents no reflection coefficient difference between the ENS "on" and "off" states. From this simulation analysis, the added uncertainty due to $\Gamma_{on/off}$ ratios is slight. If this uncertainty does prove to be substantial, one way of mitigating this effect on measurement uncertainty is to include an input fixed attenuator between the ENS and the DUT input as described in the previous section.

Excess Noise Ratio Uncertainty

Equation (5-5) defines the ENR of the ENS, from which noise source ‘hot’ temperature is calculated. ENR, which is frequency dependent, is characterized for each device by either the excess noise source manufacturer or a calibration laboratory. Measurement uncertainty during the characterization process is specified and is usually on the order of 0.2 to 0.4 dB.

Figure 6.18 shows how the ENR uncertainty adds directly to the noise figure measurement uncertainty.

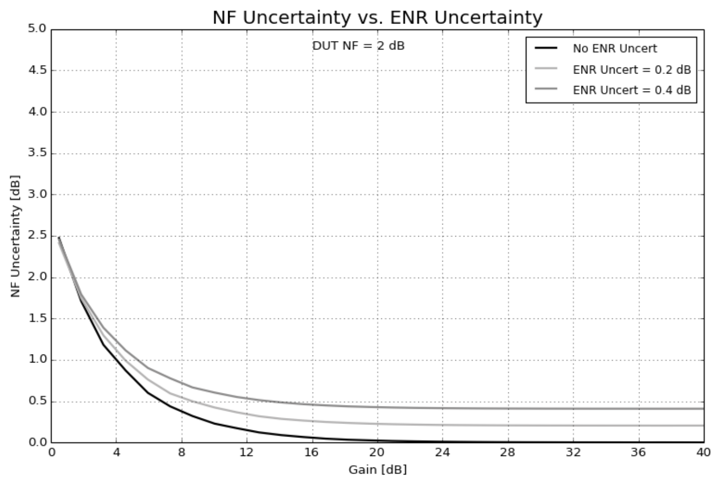

Figure 6.18 ENR Uncertainty Effect on NF Measurement Uncertainty

For instance, assuming no other uncertainties in the noise figure measurement, if the ENR measurement uncertainty is 0.4 dB, the noise figure measurement uncertainty is 0.4 dB.

Composite Noise Figure Uncertainty

Figure 6.19 shows all the uncertainties combined to arrive at the overall noise figure measurement uncertainty using the Y-factor method. The table shows the parameters used in this computation

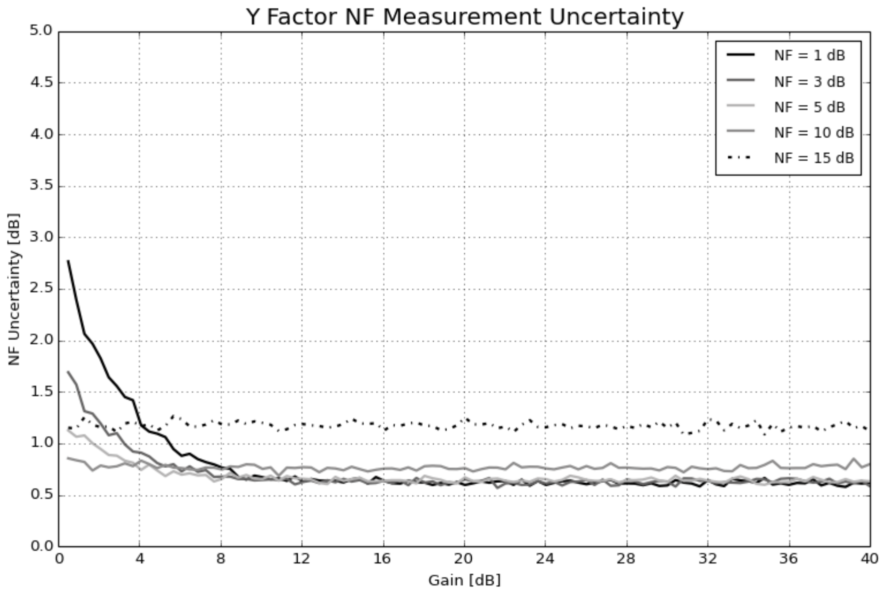

Figure 6.19 Composite Noise Figure Uncertainty

Parameter	Value	Units
DUT Input s11	-12	dB
DUT Output s22	-12	dB
Meas Receiver s11	-12	dB
Meas Receiver NF	6	dB
ENS s11	-19	dB
ENS On/Off Rho Change	0.01	--
ENR	15	dB
ENR Uncertainty	0.2	dB
Noise Measurement Variation	0.1	dB

Some observations:

- Low gain and low noise figure DUTs have the most measurement uncertainty
- Uncertainty tends to lose its dependence on DUT gain for gains greater than 10 dB
- DUTs with high noise figure have relatively high measurement uncertainty

Figure 6.20 shows the uncertainty when a 3 dB input pad is included in the Y-factor noise figure measurement.

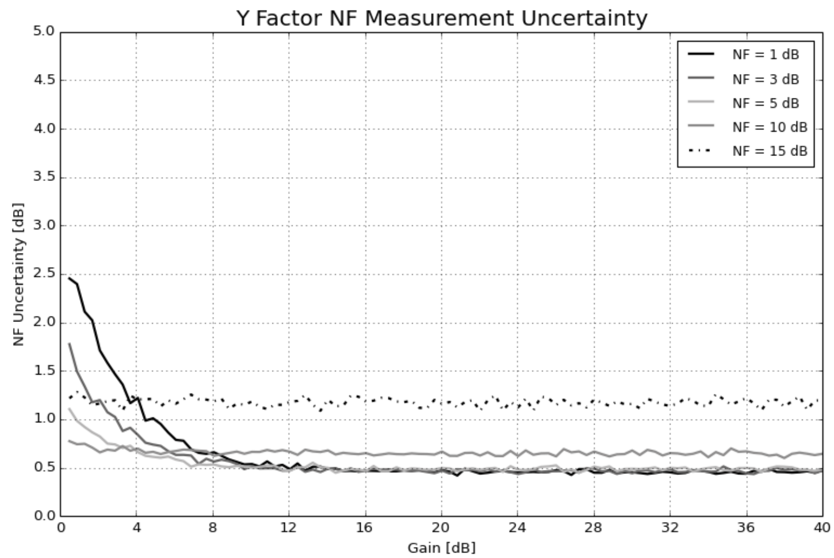

Figure 6.20 Composite Noise Figure Measurement Uncertainty with 3 dB Input Fixed Attenuator

The higher DUT gain noise figure measurement uncertainty tends to improve by about 0.1 dB to 0.2 dB with the inclusion of the input pad.

7. Cold-Source Noise Figure Measurement Technique

Observing the Y-factor measurement uncertainty versus DUT gain and DUT noise figure shown in Figure 6.19, you can notice that the Y-factor uncertainty increases as the DUT noise figure increases. For instance, the Y-factor derived uncertainty with a 15 dB noise figure DUT hovers around 1.2 dB, whereas a DUT with 3 dB noise figure has an uncertainty of around 0.6 dB. For DUTs with higher noise figures, measured noise power levels between the ENS "on" and "off" states begin to converge. The ratio of near similar noise levels for the "on" and "off" states results in increased Y-factor derived noise figure measurement uncertainty.

The cold-source technique is an alternate noise figure measurement procedure. An advantage of the cold-source technique over the Y-factor technique is reduced noise figure measurement uncertainty for high noise figure DUTs. However, cold-source relies more on the knowledge of absolute amplitude in the measurement receiver as opposed to the ratio style of the Y-factor technique which emphasizes the importance relative amplitudes. Further, cold-source requires that the DUT gain be measured outside of the noise figure measurement procedure as opposed to the Y-factor method where the DUT gain falls out of the Y-factor mathematics. Although, on the surface, cold-source appears to seem less complicated than the Y-factor method and it does allow for more accurate measurements on high noise figure devices, more care is required for the cold-source method to ensure high accuracy.

Cold-Source Measurement Procedure

The literature contains a few different variations on the cold-source measurement procedure. In many of these, a priori knowledge of the measurement receiver's noise figure is a given. In some cases the influence of the measurement receiver's noise figure is not removed from the system noise figure measurement (so-called second stage contribution) when computing the DUT's noise figure value. The cold-source technique outlined here is a two-step measurement process: step one is to measure the measurement receiver's noise figure and step two is to measure the overall DUT plus the measurement receiver system noise figure. The setups for both steps are shown in Figure 7.1:

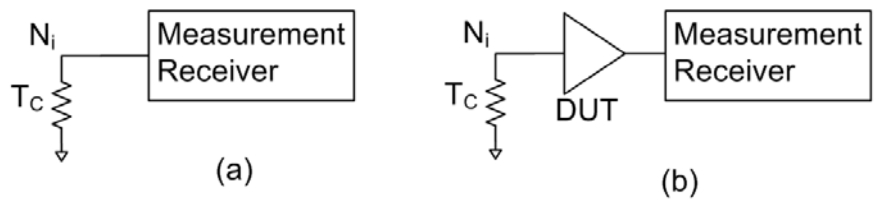

Figure 7.1 Cold-Source Measurement Setup

Both setups rely on a termination placed at the input port. This is the so-called cold-source. The nominal impedance of the termination must match those of both the DUT and the measurement receiver. To drive down the measurement uncertainty, the termination must possess a low return loss characteristic.

Step one is to measure the measurement receiver's noise figure. Equation (4-3) expressed in dB form is:

$$NF\ [dB] = N_o\,[dBm] - N_i[dBm] - G_A\ [dB] - 10\log_{10}(B) \qquad (7-1)$$

N_o is the measured noise power with the termination at the input. A generous amount of averaging as discussed in section 6 to reduce the receiver noise measurement variation is required to ensure a stable noise value. Associated gain, G_A, for a calibrated measurement receiver is 0 dB; considerations for measurement receiver amplitude accuracy -- another way of expressing the receiver's gain accuracy -- will be discussed in the next section. Bandwidth, B, is the resolution bandwidth of the measurement receiver, compensated for equivalent noise bandwidth offset. Finally, input noise, Ni, is the previously discussed kTB noise at a temperature of 290 K (-173.98 dBm/Hz).

So, for a first order approximation, to calculate the measurement receiver noise figure, measure the receiver's noise level with the input terminated normalized to a 1 Hz bandwidth. Then subtract the approximated -174 dBm/Hz kTB input noise. There are several second order effects that will increase measurement uncertainty that must be considered. These will all be discussed in the next section.

Next, the system noise figure is measured. This is the combined noise figure of the DUT plus the measurement receiver using the setup in Figure 7.1 (b). Compute the system noise figure using DUT gain (measured separately) for G_A and Equation (7-1).

The DUT's noise factor is then extracted from manipulating the cascaded noise factor equation:

$$F_{DUT} = F_{System} - \frac{F_{Receiver} - 1}{G_{DUT}} \qquad (7-2)$$

where noise factor, F, is $10^{(NF/10)}$ and the DUT's available gain, $G_{DUT,}$ is $10^{(Gain\ [dB]/10)}$. Use Equation (4-1) to convert DUT noise factor to DUT noise figure.

A word of caution is warranted at this point. The cold-source noise figure calculations outlined in this section assume matched impedances of the DUT ports, termination and measurement receiver. Measurement receiver amplitude accuracy and equivalent noise bandwidth offset were considered negligible. Termination temperature was assumed to be the defined value of 290 K. Knowledge of the

DUT's available gain (not merely the simpler s21 gain) was also assumed. Ignoring errors in any of these items leads to measured DUT noise figure uncertainty. Understanding and attempting to minimize these errors leads us into the next section.

8. Minimizing Cold-Source Measurement Uncertainty

Much like the Y-factor noise figure measurement method, the cold-source measurement method requires care in minimizing the effects that can lead to measurement uncertainty. Some of the precautions discussed in section 6 for the Y-factor method also apply to the cold-source method. *Shielding, power supply filtering*, avoiding *DUT/measurement receiver spurs*, and trace averaging to minimize *receiver noise measurement variation* all apply to the successful measurement of noise figure using the cold-source method. Additionally, the idea that the DUT noise figure itself is often dependent on the source match presented to the input of the DUT also applies. Port tuners or matching networks, as described in section 6, may be warranted to overcome this effect.

Second Stage Contribution

Second stage contribution is the term in Equation (8-1) that contains $F_{Receiver}$.

$$F_{System} = F_{DUT} + \frac{F_{Receiver} - 1}{G_{DUT}} \qquad (8-1)$$

In some implementations of the cold-source method, this term is not removed as in Equation (7-2); that is, the user makes the system noise factor measurement and considers that to be the DUT's noise factor. Figure 8.1 shows the DUT noise figure error as a function of the measurement receiver noise figure and DUT gain (DUT NF = 3 dB) when the second stage contribution is not removed.

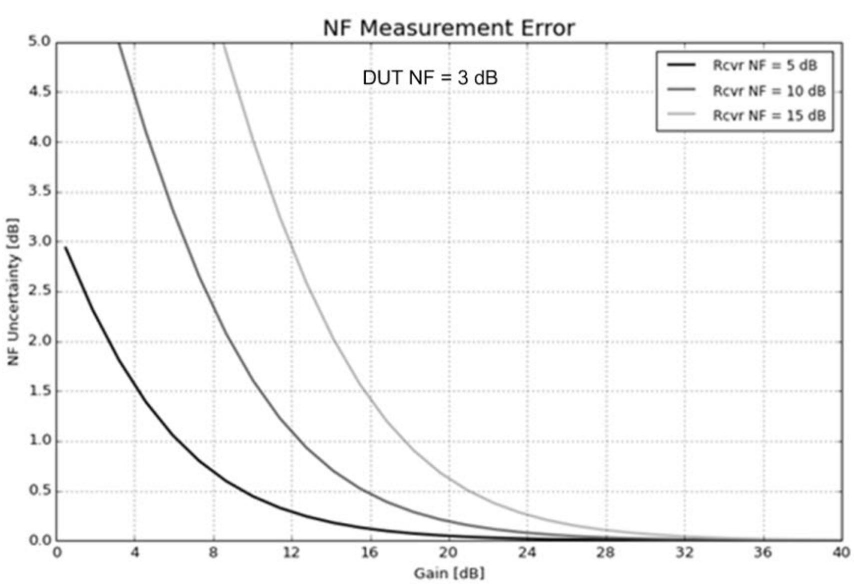

Figure 8.1 DUT NF Error vs. Measurement Receiver NF Without Removing Second Stage Contribution

Ignoring the second stage contribution to system noise figure is only appropriate for DUTs with very large gain and for measurement receivers with very small noise figure values.

Figure 8.2 shows the DUT's NF measurement uncertainty when the second stage noise figure contribution is removed. This is according to the procedure outlined in section 7 where the noise figure of the measurement receiver is measured and then applied to Equation 7-2.

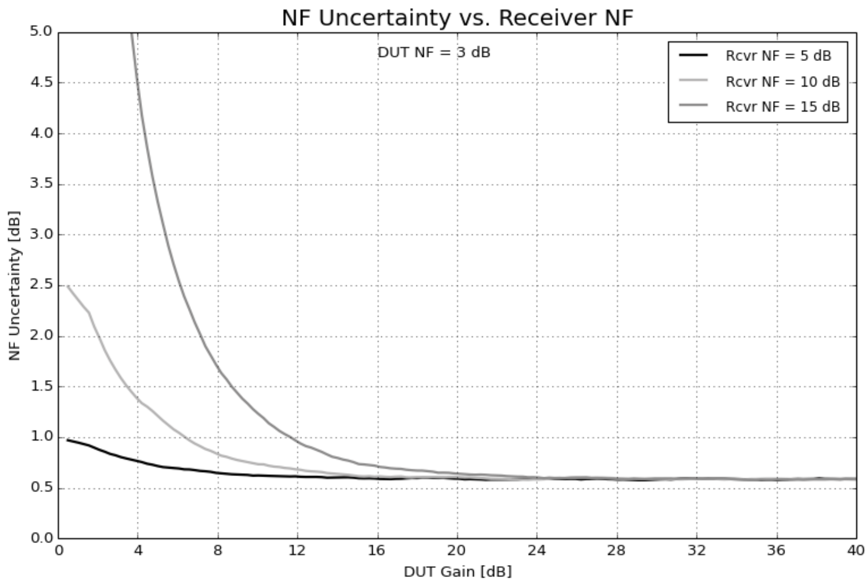

Figure 8.2 DUT NF Error versus Measurement Receiver NF without R Second Stage Contribution

In this case the DUT's NF measurement uncertainty is substantially reduced. Low DUT gain and high measurement receiver noise figure still present obstacles to achieving adequate measurement uncertainty.

Impedance Mismatch Uncertainty Considerations

In section 6, we developed much of the theory on impedance mismatch as it applies to the Y-factor technique. Nearly the same considerations concerning impedance mismatch effect on noise figure measurement uncertainty also apply for the cold-source technique.

As shown in Figure 8.3, impedance mismatch at the three interfaces of the cold-source measurement procedure contribute to the accuracy of the measured noise power used in the calculation of noise figure.

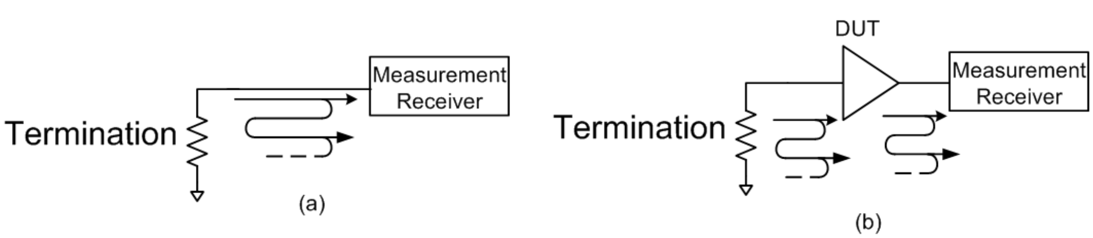

Figure 8.3 Impedance Mismatch Effects in Cold-Source Measurement

Using a high-quality termination greatly helps minimize the noise figure measurement uncertainty due to DUT and measurement receiver impedance mismatch. A termination with good return loss (> 20 dB) determines the quality of the termination.

Even with a good return loss termination, impedance mismatch at the DUT/measurement receiver port interface adds to the overall DUT noise figure measurement uncertainty. Figure 8.4 shows a similar dependence on DUT gain and noise figure for the cold-source measurement uncertainty as with the Y-factor measurement uncertainty that was presented in Figure 6.7.

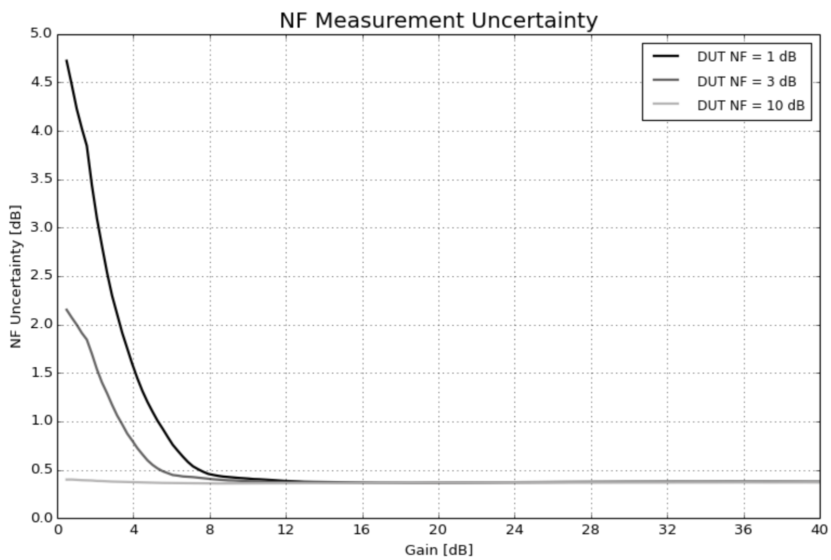

Figure 8.4 Noise Figure Measurement Uncertainty Due to Impedance Mismatch

Low DUT gain coupled with low DUT noise figure increases the noise figure measurement uncertainty that results from impedance mismatch.

Output Fixed Attenuator

For the Y-factor technique, adding fixed attenuators at either or both the input and output ports of the DUT helps improve the effective impedance match between ports. However, with a good return loss termination, there is not much room for improvement in minimizing mismatch uncertainty at the DUT input port. For this reason an input pad is not required for the cold-source technique.

Adding an output fixed attenuator between the DUT output and the measurement receiver can be considered. As in the case of the Y-factor technique, the output pad is included in the measurement of the measurement receiver's noise figure as well as the overall system noise figure. Figure 8.5 (a) shows the setup with the output fixed attenuator for part one of the cold-source measurement procedure and Figure 8.5 (b) shows the output pad for the system noise figure measurement.

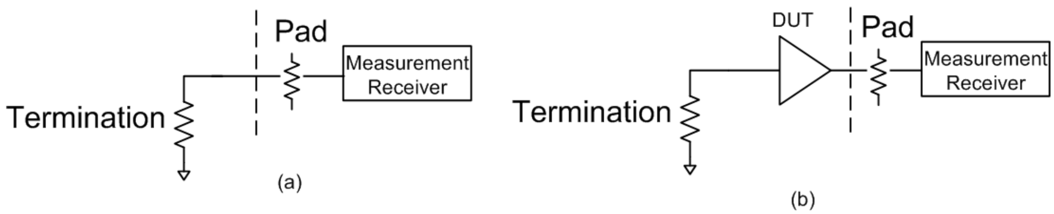

Figure 8.5 Output Pad Applied to the Cold-Source Method

Similar to the effect of the output fixed attenuator in the Y-factor technique, the cold-source also suffers the fate of degraded effective measurement receiver noise figure dominating the improvement in mismatch provided by the output attenuator. Figure 8.6 shows DUT noise figure uncertainty with and without a 3 dB output fixed attenuator in place for the cold-source measurement method.

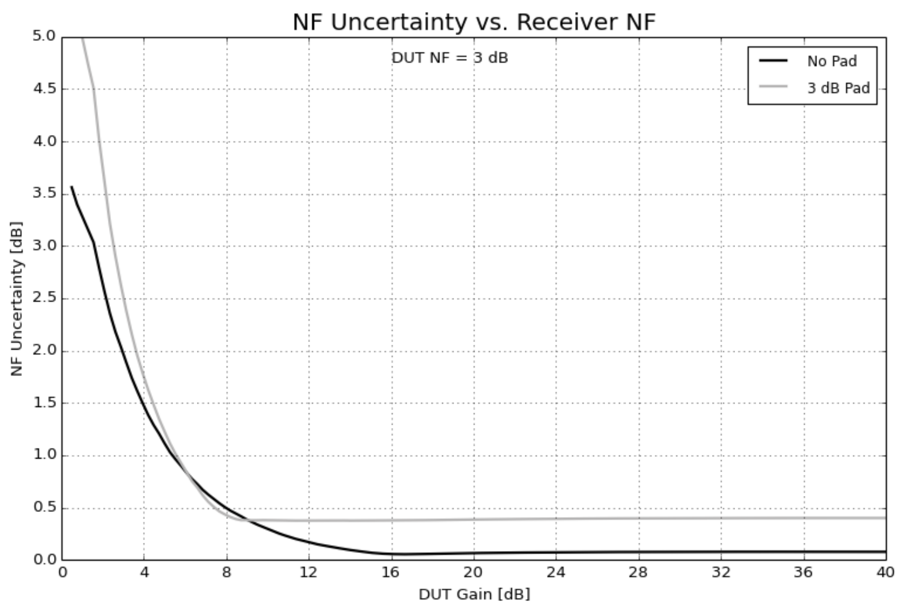

Figure 8.6 NF Uncertainty with Output Pad

Only in a narrow range of DUT gain does the fixed attenuator offer any improvement in noise figure measurement uncertainty. Over much of the DUT gain range, the degradation in measurement receiver noise figure trumps the improvement in port match with the insertion of the output fixed attenuator.

Gain Deviation Away from Available Gain

In Appendix B, three common RF power gain definitions are explained. Noise figure by definition uses available gain in its derivation. But available gain entails a conjugate match between the DUT output and the measurement receiver – achievable with either an impedance tuner or a matching circuit. The s21 power gain results from measuring the DUT with a vector network analyzer. If the DUT ports, measurement receiver input and the termination are all matched closely to 50 Ohms, then the difference between s21 gain and available gain is very slight.

Figure 8.7 demonstrates the effect on noise figure measurement uncertainty using available power gain and s21 power gain in the calculation of the DUT's noise figure (Equation 7-2).

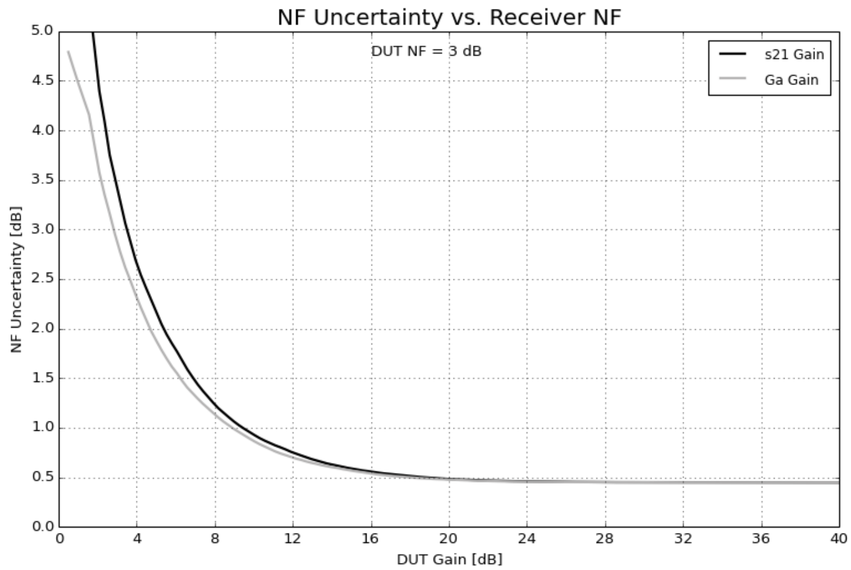

Figure 8.7 NF Uncertainty versus Power Gain Definition

At lower DUT gain, using available gain has a slight edge on using s21 power gain for measurement uncertainty. The difference is less important for DUTs with higher gain.

Measurement Receiver Amplitude Uncertainty

A measurement receiver's inability to accurately measure power can lead to a large source of noise figure measurement uncertainty. Terms such as frequency response and absolute amplitude accuracy stemming from the measurement receiver's data sheet embody the measurement receiver's amplitude accuracy performance. Since the cold-source noise figure measurement method relies on the absolute reading of noise power, any deviation in the measurement receiver's amplitude accuracy impacts the noise figure measurement result.

Figure 8.8 shows the cold-source measurement uncertainty for two levels of measurement receiver amplitude accuracy. The trace labeled '0 dB' has no measurement receiver amplitude uncertainty. The other trace has noise figure measurement uncertainty with +/- 1 of measurement receiver amplitude uncertainty.

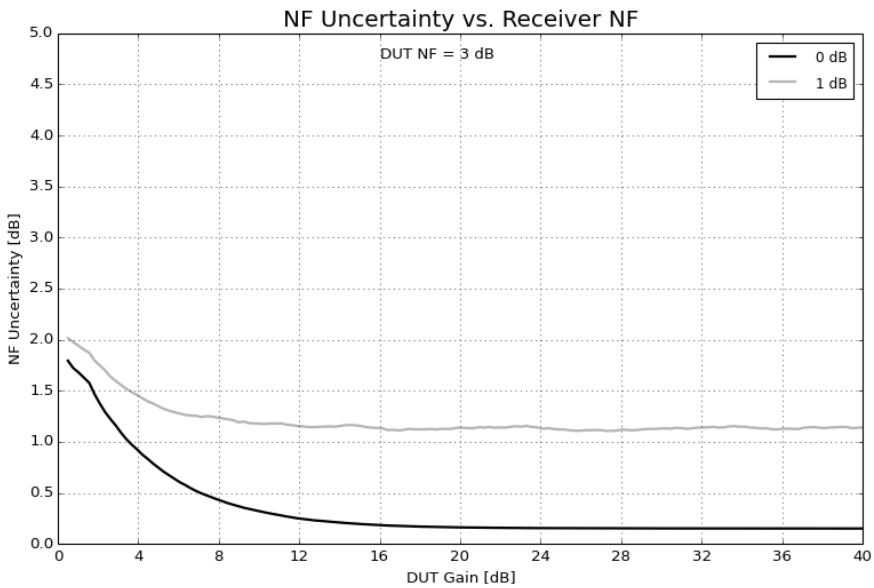

Figure 8.8 Noise Figure Uncertainty versus Measurement Receiver Amplitude Accuracy

The noise figure measurement uncertainty can rapidly deteriorate with inadequate measurement receiver amplitude accuracy.

One of the more accurate methods of minimizing the measurement receiver amplitude uncertainty is to use a power meter combined with a two-resistor power splitter as shown in Figure 8.9:

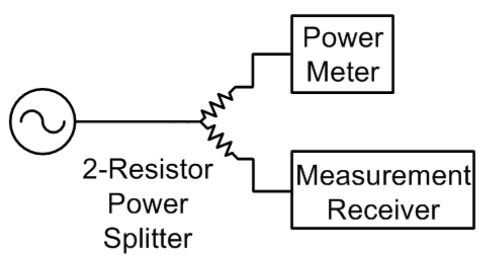

Figure 8.9 Determining Measurement Receiver Amplitude Response

References [15] and [6] clearly make the case that a two-resistor splitter as opposed to a Wilkinson power splitter or a three-resistor power splitter ensures maximum accuracy in transferring the power meter's accuracy onto the measurement receiver. The power meter absolute accuracy can be on the order of a few tenths of a dB. The two-resistor power splitter compensates the power reading for any impedance match loss at the measurement receiver's input [6].

If you go through the trouble of measuring the measurement receiver's amplitude response, one extra step can allow for the measurement of the DUT gain as shown in Figure 8.10.

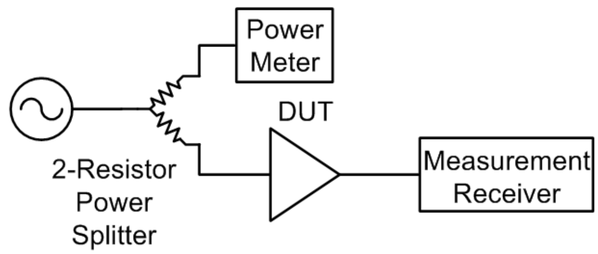

Figure 8.10 DUT Gain Measurement

Here, the measured gain is not truly available gain, which strictly speaking is the requirement for noise figure measurement, but as demonstrate above, this effect on measurement uncertainty is slight. The measurement receiver's input match is most likely not conjugately matched to the DUT. Placing a pad between the DUT and the measurement receiver improves DUT/measurement receiver mismatch uncertainty rendering the measured gain close to the s21 power gain that a vector network analyzer VNA would render.

Source Temperature Compensation

IEEE defines noise figure to be computed with a source noise temperature of 290 K (16.85 °C, 62.3 °F). Unless means are put in place to control the temperature of the termination to this defined temperature, an error will occur in the calculated noise figure when using the cold-source technique. Note: only the temperature of the termination requires the defined 290 K; the DUT and measurement receiver can operate at any desired ambient temperature.

Figure 8.11 aids in the understanding of how to compensate for the fact that the actual ambient temperature of the termination differs from 290 K, or To. Equation (2-3) already establishes the relationship between thermal noise power and temperature. In Figure 9.11, the graph shows noise power at the output of the device under test versus source temperature, Ts. This is a straight line relationship with a slope of kTsBG.

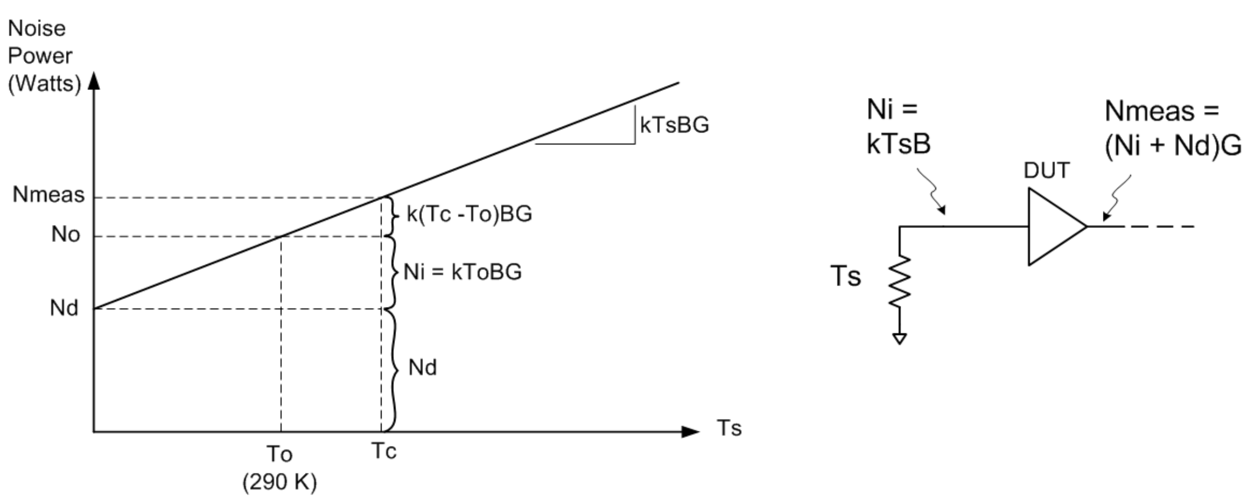

Figure 8.11 Noise Power versus Source Temperature

At source temperature equal to To, the DUT's output noise is No = (Ni + Nd)G, where input noise, Ni, is kToB and Nd is the device added noise. This is the noise power that should be used in the calculation of noise figure. However, the actual termination temperature is some arbitrary value of Tc, resulting in a noise power of Nmeas at the output of the DUT. The noise power difference between Nmeas and No is k(Tc – To)BG. Subtracting this offset from both noise measurements in the cold-source measurement procedure corrects the calculated DUT noise figure.

Figure 8.12 shows the calculated DUT noise figure error if one neglects to correct for the source temperature offset.

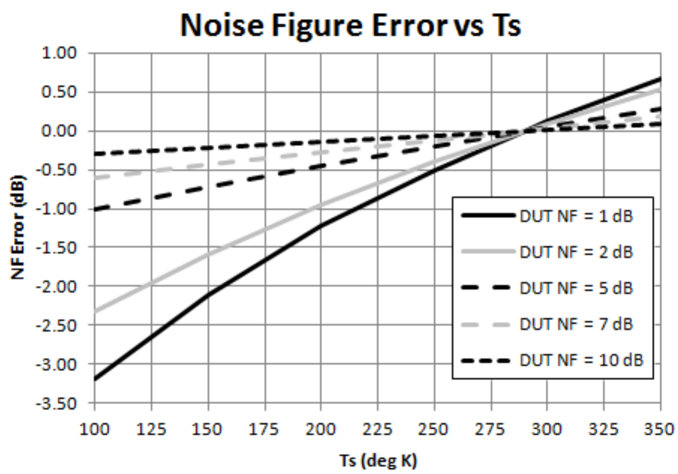

Figure 8.12 Uncompensated Noise Figure Error versus Source Temperature

Using a truly cold termination temperature (liquid Nitrogen at a boiling temperature of 77 K is one example) without applying the temperature compensation to the noise measurements can lead to substantially high noise figure measurement error.

Equivalent Noise Bandwidth Compensation

Section 3 mentions the idea that the bandwidth filter in the measurement receiver allows more noise power through than the ideal brick wall filter. This results in a noise power offset as shown in Figure 3.5. Some measurement receivers possess a noise marker that corrects for the ENBW offset. If FFT windowing is used to create the resolution bandwidth filter (RBW), one can choose the ENBW setting if available or consult tables in reference [6] to obtain the offset correction value as a function of FFT windowing type selected.

If none of the above options are available, then the offset must be determined empirically. A continuous wave (CW) source is connected to the input of the measurement receiver. For spectrum analysis where the measurement receiver is configured to display power vs. frequency, the trace can be exported directly. For time analysis where the measurement receiver is configured to display power vs. time (sometimes referred to as zero span measurement), the CW source must be stepped in frequency across the RBW filter's frequency range. At each frequency step, an amplitude measurement is made.

In either method, the data is configured as shown in Figure 8.13 showing filter response versus frequency. The amplitude data is presented in linear power terms and normalized to the maximum value.

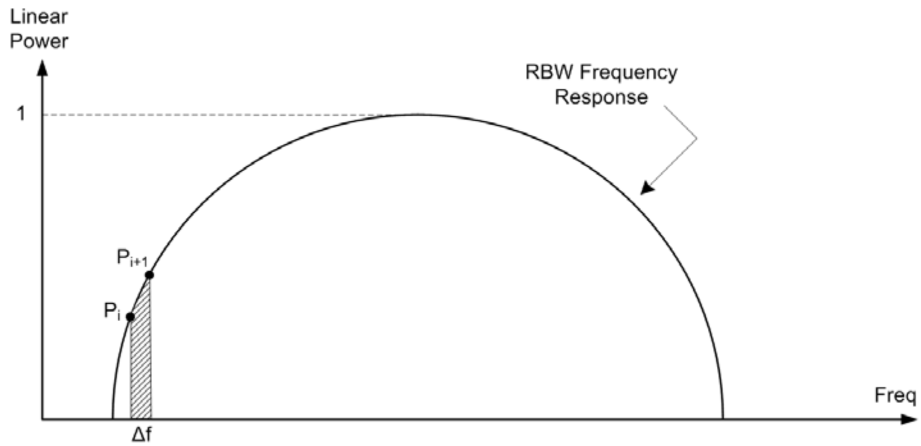

Figure 8.13 Calculation of Equivalent Noise Bandwidth Power Offset

The trapezoid method for calculating the area under the RBW is a close approximation for numerical integration:

$$P_{filter} = \sum_{i=1}^{N-1} \frac{1}{2}[P_i + P_{i+1}]\,\Delta f \qquad (8-2)$$

The ideal brick wall filter has a normalized noise power of RBW (normalized amplitude is 1 and total frequency span is the RBW filter's 3 dB bandwidth setting value).

The noise power offset due to ENBW can then be calculated as:

$$Noise\ Power\ Offset\ [dB] = 10log_{10}\left(\frac{P_{filter}}{RBW\ Setting\ [Hz]}\right) \qquad (8-3)$$

Subtract this *noise power offset* value from all noise measurement readings in the cold-source measurement procedure.

9. Measurement Uncertainty Calculation Procedure

Y-Factor Noise Figure Uncertainty Calculation Method

The literature offers several examples of noise figure measurement uncertainty analysis [13], [14]. The method used in this application note is based on the Monte Carlo technique where parameters such as port reflection coefficient phase, gain phase, noise measurement variation, ENR uncertainty, etc are randomly distributed. Noise figure is repeatedly computed using combinations of the randomly distributed parameters, which results in a probability distribution of noise figure results. From this distribution, mean and standard deviation are computed.

Power delivered to the measurement receiver uses equations stemming from signal flow graph models developed in Appendix A. Equations (A-4) and (A-5) outline the power delivered to the measurement receiver during the measurement portion of the Y-factor procedure. Equation (6-3) is used during the calibration portion of the procedure. The various port reflection coefficients are represented as complex phasors with uniformly distributed phases. On top of the reflection coefficients, normally distributed receiver noise measurement variation (display jitter), excess noise source reflection coefficient on/off ratio, excess noise source ENR error (specified by the ENS vendor), and receiver noise figure are added to the noise model.

A 1000 sample Monte Carlo type simulation is run to analyze as many possible combinations of the parameters in the model. Noise figure and gain are computed using the equations from section 5. Figure 9.1 shows noise figure measurement histogram.

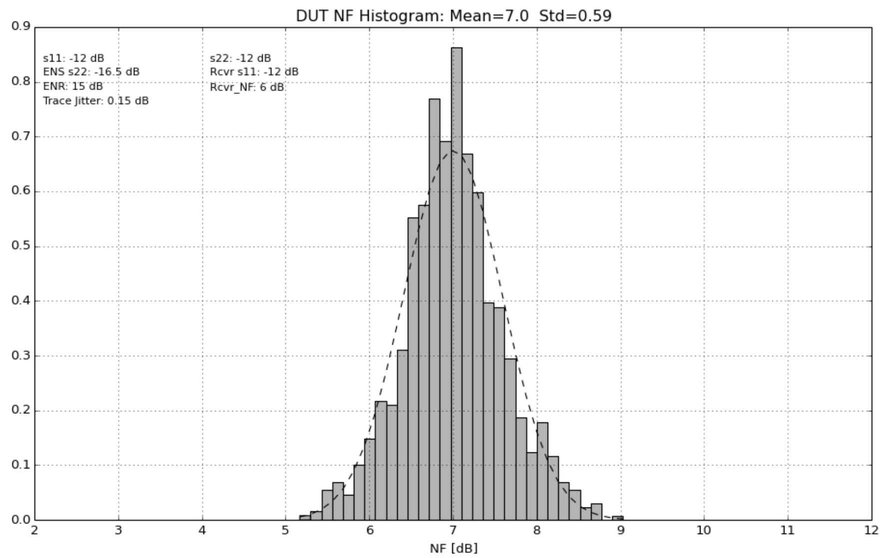

Figure 9.1 Noise Figure Measurement Histogram

True noise figure is the DUT's noise figure when all reflection coefficients are zero (perfect 50 Ω at all ports) and receiver measurement variation set to zero error. The difference between the computed noise figure mean and the true noise figure +/- 2 standard deviations is considered the measurement uncertainty. With uncertainty calculated in this manner, 95% of the computed noise figure values will fall within this uncertainty range. Measurement uncertainty computed in this manner is reported in the graphs in section 6.

Gain error is considered to be the difference between measured gain and computed available gain. Available gain, gain where the DUT's output is conjugately matched to the load, is discussed in Appendix B. Again a two sigma value is considered as the gain measurement error. An example of gain error distribution is shown in Figure 9.2.

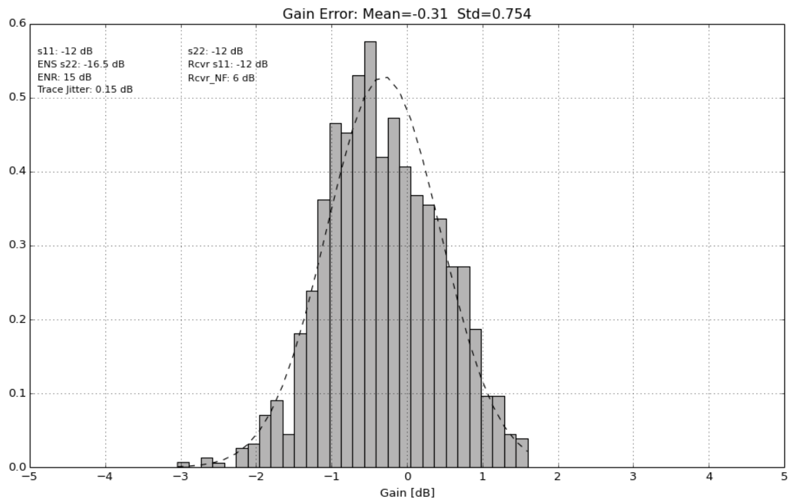

Figure 9.2 Gain Error Histogram

Cold-Source Uncertainty Calculation Method

A similar approach to the Y-factor uncertainty calculation is also used for the cold-source technique. The two-step measurement approach outlined in section 7 is used in the calculations. Parameters including DUT scattering parameter phases, measurement receiver amplitude accuracy, receiver noise measurement variation, etc are randomly distributed and used in a Monte Carlo type simulation.

NI Noise Figure Uncertainty Calculator

The uncertainty calculation methods outlined above lay at the heart of the uncertainty calculator in the National Instruments noise figure measurement application software. Both the Y-factor and cold-source noise figure measurement uncertainties are calculated in this utility. Figure 9.3 shows the front panel of the uncertainty calculator for the Y-factor method.

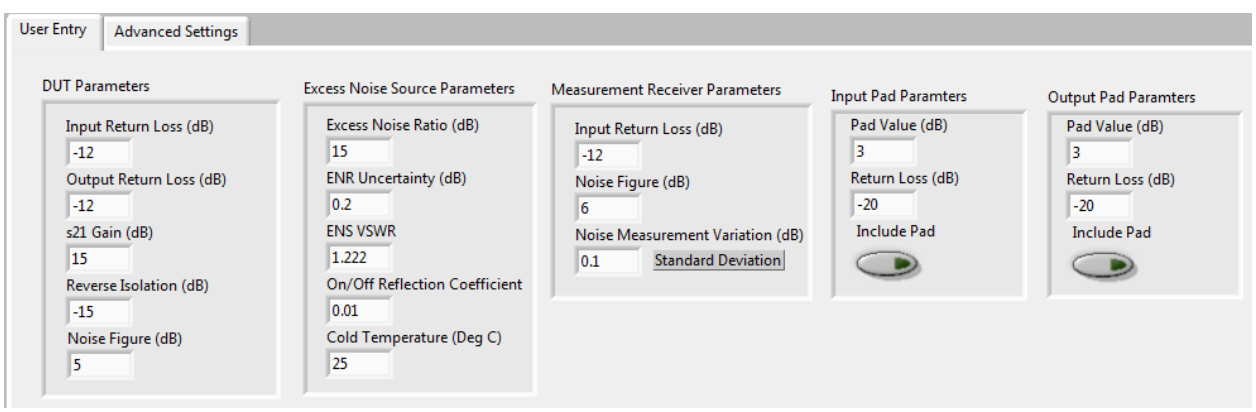

Figure 9.3 Noise Figure Uncertainty Calculator Front Panel

The uncertainty is calculated at a single measurement frequency. The “User Entry” tab allows for input of DUT, Measurement Receiver and Excess Noise Source parameters. Input and Output Fixed Attenuator can also be incorporated into the uncertainty calculation using this tab.

The ‘Advanced Settings’ tab, shown in Figure 9.4, allows for toggling on and off parameters used for the Monte Carlo analysis.

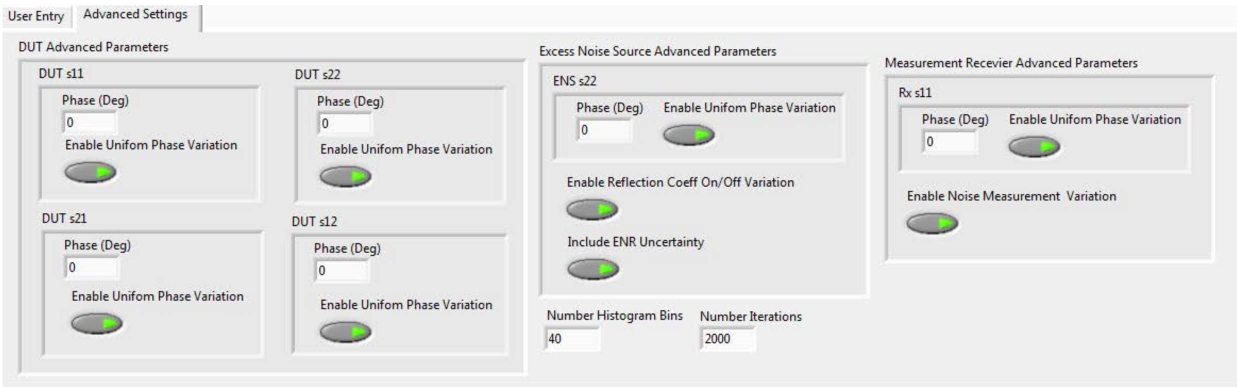

Figure 9.4 Advanced Settings Tab

For instance, if a certain parameter is enabled with the associated Boolean toggle button, then a probability distribution is generated for that parameter. Otherwise, a constant value is used for that parameter.

The results are shown as histograms as shown in Figure 9.5:

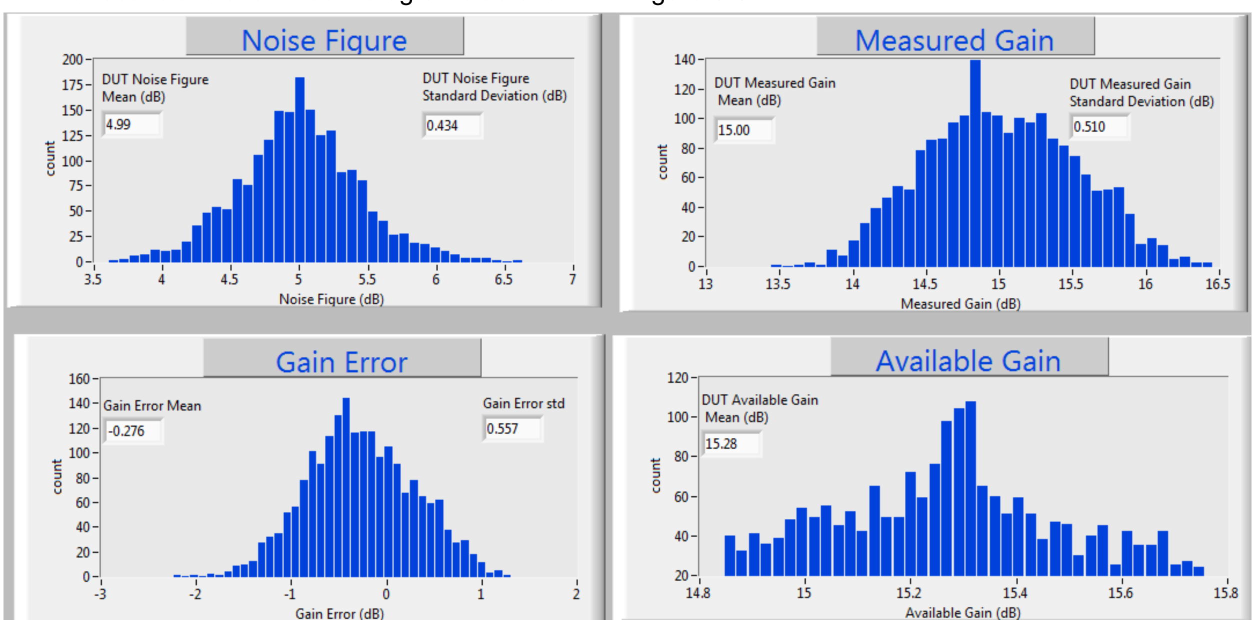

Figure 9.5 Uncertainty Results

Viewing the histograms of computed noise figure, measured gain and gain error allows for the inspection of how closely the data resembles a normal distribution. With a normal distribution, confidence levels based on standard deviation have relevancy.

10. Summary

This application note has introduced noise figure measurement as applied to RF circuits and systems. First topic was the sources of noise. Following this was a treatment of noise in a cascade of RF components. Next the theory of two particular noise figure measurements(the Y-factor method and the cold-source method) was developed. For both noise figure measurement methods, considerations for the measurement uncertainty; both the source of uncertainty and ideas on minimizing uncertainty were discussed.

Appendix A: Signal Flow Graphs

For details on scattering parameters (S-parameters) and signal flow graphs, reference [10] should be consulted. This appendix summarizes these concepts for use in noise figure equations.

For RF circuits, calculations concerning power flow dominates over calculations that use voltages and currents at any given circuit node. Power flow along a transmission line consists of incident and reflected power flow components. S-parameters provide a convenient way of analyzing RF circuits based on power flow. Vector Network Analyzers are designed to measure S-parameters of devices for use in RF circuit analysis. Figure A.1 along with Equations (A-1) and (A-2) define normalized incident and reflected voltages.

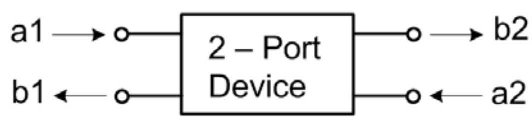

Figure A.1 Incident and Reflected Normalized Voltages

$$a_x = \frac{V_{incident}}{\sqrt{Z_x}} \qquad b_x = \frac{V_{reflected}}{\sqrt{Z_x}} \tag{A-1}$$

$$|a|^2 = incident\ power \qquad |b|^2 = reflected\ power \tag{A-2}$$

Normalized voltages ‘a’ signify incident normalized voltage into the port and normalized voltages ‘b’ signify reflected normalized voltage out of the port. Incident and reflected powers are the magnitude squared of either ‘a’ or ‘b’. The normalizing impedance, Zx, is generalized to be the characteristic impedance of the input and output ports, which are not necessarily the same. Most often the characteristic impedance of the two ports are the same and are typically 50 Ω.

Figure A.2 shows that the normalized incident and reflected port voltages are used to construct the scattering matrix.

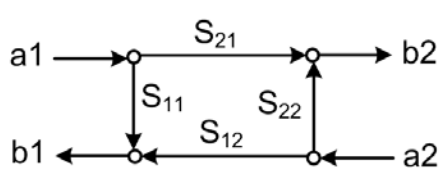

$$\begin{bmatrix} b1 \\ b2 \end{bmatrix} = \begin{bmatrix} S_{11} & S_{12} \\ S_{21} & S_{22} \end{bmatrix} \begin{bmatrix} a1 \\ a2 \end{bmatrix}$$

Figure A.2 Scattering Parameters

S_{11} and S_{22} are the input and output port reflection coefficients. These are measured by terminating the opposite port in the characteristic impedance of the system, Zo. S_{21} and S_{12} are the forward and reverse transmission coefficients, measured with the output and input port respectively terminated in the characteristic impedance of the system.

Although S-parameters are relatively easy to measure and are commonly supplied by device manufactures, they cannot be directly cascaded. One must resort to using Mason’s Rule [10] to determine the various port powers in a system consisting of cascaded blocks that are represented using

S-parameter data. Mason's Rule is greatly facilitated by the use of signal flow graphs. Figure A.2 represents the signal flow graph of a two-port device. Figure A.3 shows the signal flow graph when the two-port device is connected to an input signal generator and an output load.

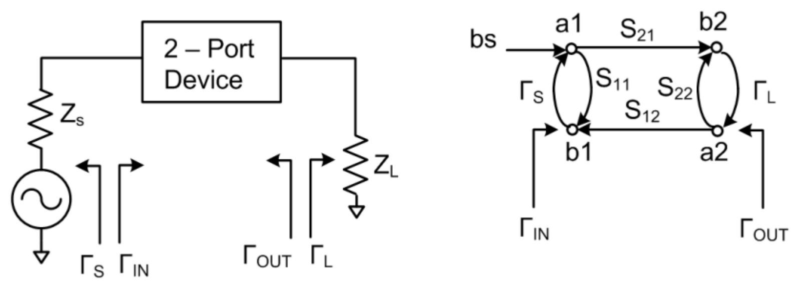

Figure A.3 Signal Flow Graph of a Two-Port Device

The arrows in the signal flow graph represent power flow into and out of the ports. The source and load impedances also have reflection coefficients. The reflection coefficients of the input and output terminations follow Figure A.4 and Equation (A-3):

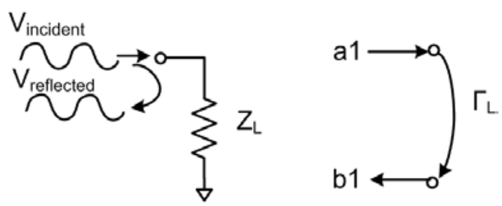

Figure A.4 Reflection Coefficient

$$\Gamma_L = \frac{Z_L - Z_0}{Z_L + Z_o} \quad \text{(A-3)}$$

Power delivered to the load is given by:

$$P_L = |b_2|^2 - |a_2|^2 = |b_2|^2(1 - |\Gamma_L|^2) \quad \text{(A-4)}$$

To compute the reflected normalized voltage out of port 2 of the device, b2, we must resort to Mason's Rule (see reference [10]). In this example, b2 is given by:

$$b_2 = \frac{S_{21} b_S}{1 - (S_{11}\Gamma_S + S_{22}\Gamma_L + S_{21}\Gamma_S S_{12}\Gamma_L) + S_{11}\Gamma_S S_{22}\Gamma_L} \quad \text{(A-5)}$$

Each term in equation (A-5) is complex. Complicating matters further is that the magnitude and phases of each term vary with frequency. Most often the exact phases are not completely predictable in an actual circuit implementation in which case the terms in the denominator become uncertainties.

Figure A.5 shows a more realistic circuit where transmission lines connect adjacent stages in a system.

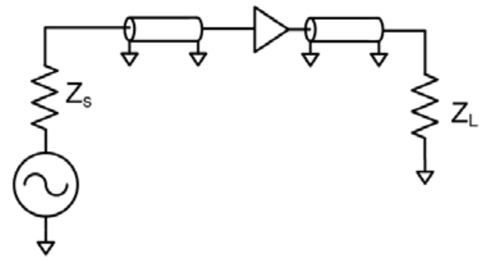

Figure A.5 Circuit with Transmission Lines

When impedances are not matched at each device port, the transmission lines create a frequency dependent phase that when using equations (A-4) and (A-5) to determine power delivered to the load, a power error results as shown in Figure A.6. Unless the complex S-parameters of each device, including the transmission lines, are known, the power error at any given frequency will not be known. Only the range of power error can be anticipated.

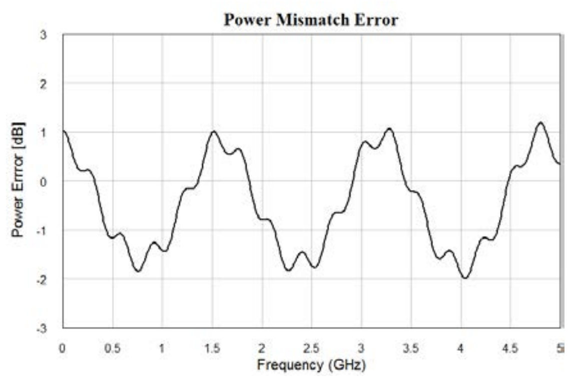

Figure A.6 Power Error with Circuit Impedance Mismatches

The conclusion is that achieving maximum power transfer by means of matching impedances between stages is important in RF design. When impedances are not matched, anticipating the errors in the power delivered to the load requires a complicated analysis procedure involving signal flow graphs and Mason's Rule.

Appendix B: Power Gain Equations

Transducer Power Gain and Available Power Gain

There are a few different methods of specifying power gain in RF circuits. Two of the power gain equations that are important for noise figure calculation are: *transducer power gain*, G_T and *available power gain*, G_A. These different power gain definitions are given in reference [11]:

$$G_T = \frac{P_{DEL}}{P_{AVS}} = \frac{\textit{Power delivered to the load}}{\textit{Power available from the source}}$$

$$G_A = \frac{P_{AVN}}{P_{AVS}} = \frac{Power\ available\ from\ the\ network}{Power\ available\ from\ the\ source}$$

Both equations have *power available from the source*, P_{AVS}, in the denominator. Power available from the source is another term for maximum power transfer from the source. Earlier it was mentioned that if the real impedances of the source and load are equal, then maximum power transfer occurs. This needs to be generalized for complex impedance. Maximum power transfer occurs when the load impedance is a conjugate match to the source impedance as shown in Figure B.1:

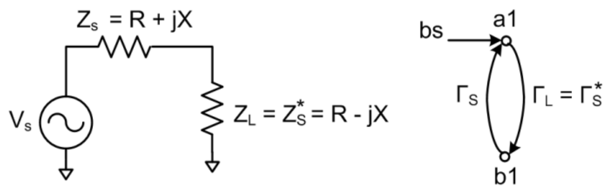

Figure B.1 Conjugate Matched Source

Complex impedance will also have complex reflection coefficient. Conjugate match also means that the reflection coefficient of the load is conjugate to the reflection coefficient of the source. Power available from the source using Figure B.1 is:

$$P_{AVS} = |a_1|^2 - |b_1|^2 = |a_1|^2(1 - |\Gamma_s|^2) \qquad \text{(B-1)}$$

Using signal flow graphs and Mason's Rule:

$$a_1 = \frac{b_S}{1 - \Gamma_S \Gamma_S^*} = \frac{b_S}{1 - |\Gamma_S|^2} \qquad \text{(B-2)}$$

Thus,

$$P_{AVS} = \frac{|b_S|^2}{1 - |\Gamma_S|^2} \qquad \text{(B-3)}$$

For transducer power gain, the power delivered to the load is given by Equation (A-4). Plugging (A-5) into (A-6) and using Equation (B-3), G_T is given by:

$$G_T = \frac{1 - |\Gamma_S|^2}{|1 - S_{11}\Gamma_S|^2} |S_{21}|^2 \frac{1 - |\Gamma_L|^2}{|1 - \Gamma_L \Gamma_{OUT}|^2} \qquad \text{(B-4)}$$

where Γ_{OUT} is the reflection coefficient looking into the output port of the two-port device (see Figure A.3). Formally, Γ_{OUT} is given by:

$$\Gamma_{OUT} = S_{22} + \frac{S_{12}S_{21}\Gamma_S}{1 - S_{11}\Gamma_S} \qquad \text{(B-5)}$$

Available power gain, G_A, is transducer power gain under the condition that Γ_{OUT} is conjugately matched to the load reflection coefficient, Γ_L.

$$G_A = \frac{1-|\Gamma_S|^2}{|1-S_{11}\Gamma_S|^2}|S_{21}|^2\frac{1}{1-|\Gamma_{OUT}|^2} \quad \text{(B-6)}$$

The implication of Equation (B-6) is that the output impedance of each stage in a cascade must be conjugately matched to the input impedance of the following stage.

Figure B.2 shows how to design a cascade of individual devices with available gain in mind.

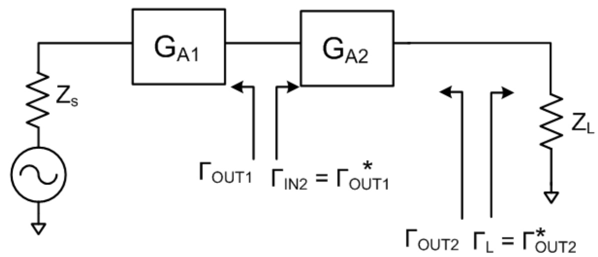

Figure B.2 Available Cascaded Power Gain

Designing with conjugate matching is difficult to implement especially over a broad frequency range. One method of designing to available gain is to ensure all output and input impedances equal the characteristic impedance of the system (typically 50 Ω). Figure B.3 shows one technique that uses inter-stage matching networks to ensure proper impedances in the chain.

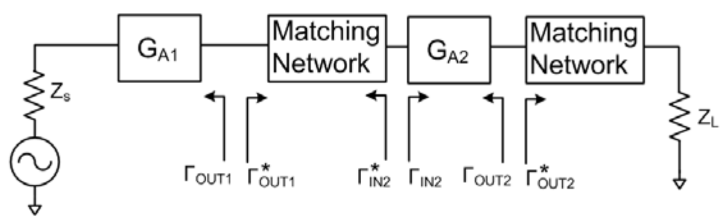

Figure B.3 Designing a Cascade for Available Power Gain

Figure B.4 shows a comparison between available power gain and transducer power gain as a function of load return loss and two-port device output return loss.

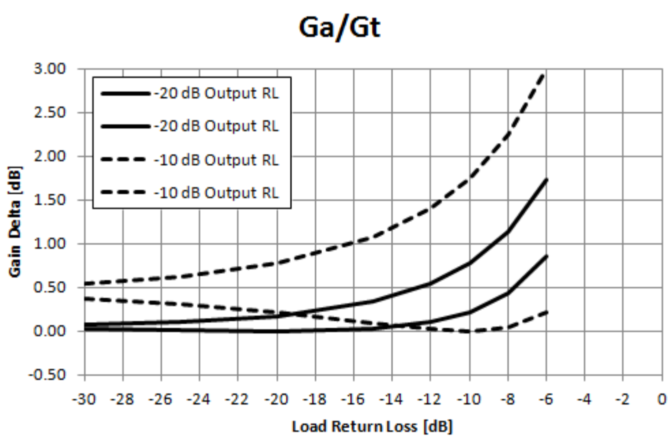

Figure B.4 Available Power Gain versus Transducer Power Gain

Available power gain always exceeds transducer power gain and there is a range of gain differences depending on the relative phase relationship between Γ_{OUT} and Γ_L . One could view this graph as the error incurred assuming available power gain when the circuit is not designed for conjugate matching between device output and the load.

When one designs for available power gain, then the total available power gain of the system is simply:

$$G_{A\,total} = G_{A1}G_{A2}G_{A3} \dots \tag{B-7}$$

Applying noise figure in a cascade, such as Friis' cascaded noise figure in Equation (4-10) assumes available power gain. If the output impedances of the stages are not conjugately matched to their load impedances, then the simple system gain equation in Equation (B-7) does not apply and a more complicated approach involving signal flow graphs becomes a requirement.

Operating Power Gain

Operating power gain makes no assumptions about conjugate matching at the port planes. Operating Power Gain is given by Equation (B-8):

$$G_P = \frac{P_{DEL}}{P_{IN}} = \frac{Power\ delivered\ to\ the\ load}{Power\ input\ to\ the\ device} \qquad (B-8)$$

In terms of DUT S-parameters and load reflection coefficient:

$$G_P = \frac{1}{1-|\Gamma_{IN}|^2}|s_{21}|^2\frac{1-|\Gamma_L|^2}{|1-S_{22}\Gamma_L|^2} \qquad (B-9)$$

Where,

$$\Gamma_{IN} = s_{11} + \frac{S_{12}S_{21}\Gamma_L}{1-S_{22}\Gamma_L} \qquad (B-10)$$

s21 Power Gain

When a vector network analyzer (VNA) is used to measure the gain of a device, the gain measured is the s21 gain. Appendix A introduces the concept of S-parameters. Using this foundation, s21, or forward transmission coefficient, is defined as:

$$S_{21} = \left.\frac{b_2}{a_1}\right|_{a_2=0} \qquad (B-11)$$

The restriction that the output incident normalized voltage equals zero demands that the output port be terminated in the nominal impedance of the system (usually 50 Ohms). Power gain is then the magnitude of S_{21} squared:

$$G_{S_{21}} = |S_{21}|^2 \qquad (B-12)$$

Equations (B-4) for transducer power gain and (B-6) for available gain show that s21 power gain is part of the definitions of these power gains. In most cases the s21 power gain is the lowest of the three power gains described in this appendix as demonstrate in Figure B.5:

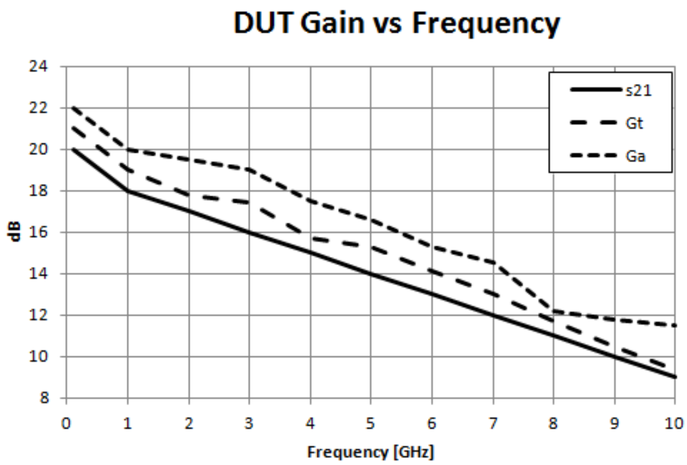

Figure B.5 Amplifier Power Gain versus Frequency

As the return loss of the DUT, source and load improve, the three gain values begin to converge.

The main consideration to be taken away from this appendix is that multiple definitions apply to the term power gain. Most commonly, s21 power gain is assumed to be the DUT's power gain as this is the value measured. Available power gain, however, is the gain used in the definition of noise figure.

Appendix C: Effective Noise Temperature

A term often associated with noise figure is *effective noise temperature.* Effective noise temperature, Te, is an alternate way of expressing the noise contribution of a device. For space-based applications, the input noise levels to the antenna become extremely small. Using the relation Ni = kTB to describe input noise power, the space-based applications have a *noise temperature* of a few kelvin as opposed to the common 290 K noise temperature used in the definition of noise figure. Device noise figures used in these applications become much, much less than 1 dB. Using effective noise temperature to describe device noise characteristics becomes more convenient than noise figure.

Consider Figure C.1 for the development of the concept of effective noise temperature:

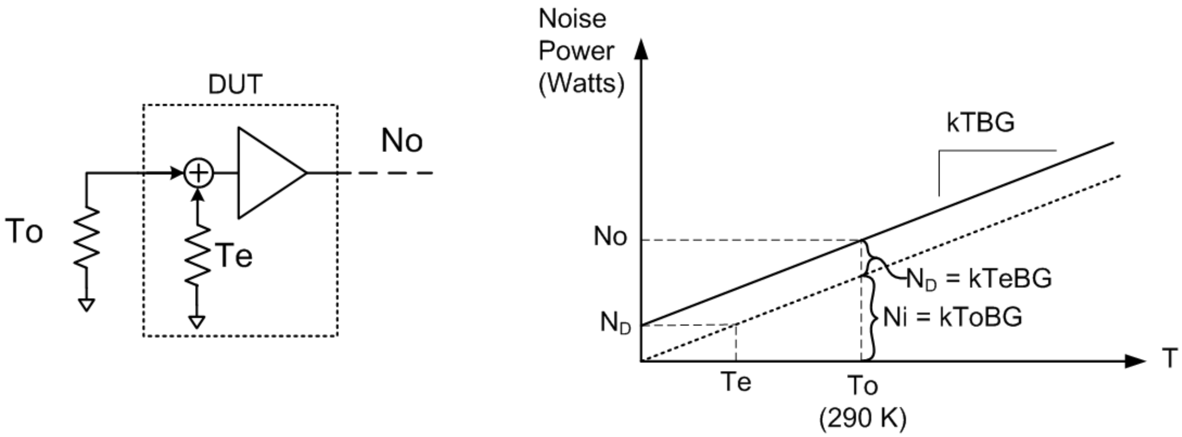

Figure C.1 Effective Noise Temperature

The device-added noise, N_D, can be modeled as summing a resistor with a noise temperature of Te at the input of a noise-free device. Device added noise is then:

$$N_D = kT_eB \qquad (C-1)$$

Input noise, Ni, is defined as noise at a temperature of To = 290 deg K. At the device output, the noise power is given as:

$$N_0 = (N_i + N_D)G_A = kG_AB(T_o + T_e) \qquad (C-2)$$

Equation (C-2) demonstrates how noise temperatures can be combined in a system as opposed to noise factors. Using the definition of noise factor from Equation (4-6), noise factor in terms of effective noise temperature is:

$$F = 1 + \frac{N_D}{kT_oB} = 1 + \frac{T_e}{T_o} \qquad (C-3)$$

A cascade of devices, each characterized with their own effective noise temperature, has an overall system noise temperature given by:

$$T_e = T_{e1} + \frac{T_{e2}}{G_{A1}} + \frac{T_{e3}}{G_{A1}G_{A2}} + \cdots \qquad (C-4)$$

References

[1] Henry W. Ott, *Noise Reduction Techniques in Electronic Systems*, 2nd ed., 1988.
[2] J.B. Johnson, "Thermal Agitation of Electricity in Conductors", *Physics Review,* July 1928.
[3] Paul Gray, Robert Meyer, et al., *Analysis and Design of Analog Integrated Circuits,* 5th ed., 2009.
[4] *Noise Specs Confusing?*, Application Note AN-104, National Semiconductor.
[5] Simon Haykin, *Communications Systems*, 2nd ed., 1983.
[6] *Super-Heterodyne Signal Analyzers*, NI
http://ftp.ni.com/evaluation/rf/Super_Heterodyne_Signal_Analyzers.pdf
[7] IRE Subcommittee 7.9 on Noise, "Description of Noise Performance of Amplifiers and Receiving Systems", Proceedings of the IEEE, March 1963.
[8] H.T. Friis, "Noise Figure of Radio Receivers", Proceedings of the IRE, July, 1944.
[9] *Modern RF and Microwave Measurement Techniques*, 2013
[10] *S-Parameter Design*, Application Note 154, Hewlett-Packard Company.
[11] G. Gonzalez, *Microwave Transistor Amplifiers*, 1984.
[12] Richard Lyons, *Understanding Digital Signal Processing,* 2001.
[13] *Modern RF and Microwave Measurement Techniques*, 2013.
[14]N. Otegi, et. al., "Statistical Analysis of Accuracy in Noise Figure Measurements", 66th ARFTG Microwave Measurements Symposium.
[15] R. Johnson, "Understanding Microwave Power Splitters", Microwave Journal, Dec. 1975.